TVS-CV-82-108
UTIAS Report No. 263

The Obstacle Avoidance Manoeuvre as Performed in a Tractor/Semitrailer Truck

L.D. Reid
Associate Professor

W.O. Graf
Research Engineer

University of Toronto
Institute for Aerospace Studies

A.M. Billing *
Research Officer
Transport and Vehicle Systems
Research and Development Branch, MTC

*Mr. Billing is now with Arcon Engineering Consultants Ltd.

Published by:
The Policy Planning and Research Division
Ontario Ministry of Transportation and Communications
Hon. James W. Snow, Minister
H.F. Gilbert, Deputy Minister

Published without prejudice
as to the application of the findings.
Crown copyright reserved; however, this
document may be reproduced for non-commercial
purposes with attribution to the Ministry.

For additional copies write:
The Editor
Research and Development Branch
Ministry of Transportation and Communications
1201 Wilson Avenue
Downsview, Ontario
M3M 1J8

June 1982

ABSTRACT

A series of field trials was carried out employing an instrumented tractor/semitrailer truck and an obstacle avoidance manoeuvre. Driver/vehicle response records were taken and used as input to a driver model fitting computer algorithm. Linear driver models were successfully fitted to the experimental data and the resulting model parameters are presented. These results span a number of task conditions ranging from very easy to quite demanding.

ACKNOWLEDGEMENTS

This study was prepared with the support of the Research and Development Branch of the Ontario Ministry of Transportation and Communications under the Ontario Joint Transportation and Communications Research Programme, Contract No. 31614. The authors would also like to thank General Motors for providing the lane tracking equipment and additional financial support. Thanks also to the four Ministry drivers and other Ministry personnel who assisted in running the field trials.

CONTENTS

PAGE

ABSTRACT ii

ACKNOWLEDGEMENTS iii

NOTATION vi

1/ INTRODUCTION 1

2/ VEHICLE, TEST SITE, AND DRIVING TASKS 2
2.1/ Vehicle Characteristics 2
2.2/ Test Site 2
2.3/ Driving Tasks 3

3/ INSTRUMENTATION 5
3.1/ Sensors 5
3.2/ Data Acquisition System (DAS) 6
3.3/ Data Handling 8

4/ DRIVER MODEL 10

5/ EXPERIMENTAL DETAILS 11
5.1/ Subjects. 11
5.2/ Training. 11
5.3/ Production Runs 12
5.4/ General Procedures. 12

6/ DATA ANALYSIS 13
6.1/ Driver Model Fitting Technique. 13
6.2/ Input Data Files. 15

7/ DISCUSSION OF RESULTS 18
7.1/ Training Effects. 18
7.2/ The Model Fitting Process 19

PAGE

8/ SUMMARY 24

REFERENCES 25

TABLES 26

FIGURES 36

APPENDIX A/ Lane Tracker Measurements 57

APPENDIX B/ Active Pole Triggering Mechanism 63

APPENDIX C/ Instructions to Drivers 66

NOTATION

$\underline{A}$ linear model state matrix with elements A_{ij}

$\underline{b}$ driver model constant output offset vector

$\underline{B}$ linear model input distribution matrix with elements B_{ij}

$\underline{c}$ vector of linear model parameters

$\underline{D}$ weighting matrix in the expression for J

$\underline{e_I}$ unit vector pointing from the lane tracker to the road centre stripe with components in F_I of $(e_{11}\ e_{12}\ e_{13})$

F_B body-fixed reference frame

F_C lane tracker-fixed reference frame

F_I road-fixed reference frame with x-axis aligned with centre stripe

G_ψ driver model gain (degrees/degree)

J model fitting algorithm cost functional

$\underline{L}_{xy}$ transformation matrix from F_y into F_x

$\underline{0}$ the null matrix

s the Laplace variable, or the distance travelled by the tractor as measured by road wheel revolutions (according to context)

t time

T recorded data record length

T_I driver model lag time constant (seconds)

T_L driver model lead time constant (seconds)

$\underline{u}$ linear model control input vector

V vehicle forward speed

(x,y,z) coordinates of the tractor's centre of gravity in the road-fixed reference frame F_I, y positive to the right

(x_b,y_b,z_b) the origin of F_B in F_I coordinates

(x_c,y_c,z_c) the origin of F_C in F_I coordinates

(x_d,y_d,z_d) the origin of F_C in F_B coordinates

$\underline{x}$ linear model state vector

$\underline{y}$ linear model response vector

y_o distance from end of obstacle pole to the Phase I sight point

$\underline{z}$ experimentally-measured system response vector

z_{cg} the Z-coordinate of the tractor's centre of gravity in F_B coordinates

β lane tracker angular output

δ_s steering wheel angle, positive to the right

$\delta_{s\tau}$ steering wheel angle advanced in time by τ seconds

$\Delta\%$ percent change in driver model parameter

$\Delta J\%$ percent change in J

$\Delta_c J$ gradient of J with respect to $\underline{c}$

ΔS sight point shift in Phase II corresponding to nonzero $\underline{b}$ value

Δt sampling interval

Δt_l time spent in passing lane by the tractor's centre of gravity

(θ, ϕ, ψ) Euler angles relating F_B to F_I

τ driver model time delay

τ_R driver's initial reaction time to the falling of the obstacle pole

ϕ tractor's roll angle with respect to the gravity vector, positive to the right

ψ tractor's heading angle with respect to the road centre strip, positive to the right

ψ_t sight point angle, see Figure 4.1

VECTORS, MATRICES AND OPERATORS

$\dot{x}$ time derivative of x(t)

$\bar{x}$ Laplace transform of x(t)

$\underline{x}$ vector (or column matrix)

$\underline{A}$ matrix with the element A_{ij} in the ith row and jth column

$\underline{A}^T$ the transpose of $\underline{A}$

1/ INTRODUCTION

The obstacle avoidance manoeuvre is one which can lead to vehicle loss of control under certain conditions. For this reason it represents a reasonable starting point in a study aimed at analyzing driver/vehicle performance. Reference 1 describes a series of driving simulator tests performed as part of this study. The present report describes a series of field trials carried out as an extension to this work. The full-scale test program was undertaken in order to generate data for the development of driver models applicable to obstacle avoidance manoeuvres performed in a tractor/semitrailer truck. It was conducted at the Ministry of Transportation and Communications' (MTC) Huron Park test facility. Driver/vehicle responses during a number of test manoeuvres (based on a pole that could be made to fall at a controlled distance in front of the vehicle) were recorded using on-board instrumentation linked by telemetry to a laboratory recorder. The data from selected runs were reduced into a form suitable for analysis. Linear driver models were then fitted to the test results by using the computer algorithm described in Reference 2.

2/ VEHICLE, TEST SITE, AND DRIVING TASKS

2.1/ Vehicle Characteristics

The test vehicle was a 1975 White Freightliner cab-over-engine tandem axle tractor and a tandem axle flatbed semitrailer carrying a 7700 kg load of concrete ballast on all test runs (see Figure 1). The vehicle specifications are given in Table 1 and Figure 2.

The flatbed semitrailer was of the trombone type, operated fully extended at a length of 9.58 m. The fifth wheel was mounted very close to the midpoint of the tractor's rear axles. Safety cables joining the tractor and the semitrailer limited the maximum articulation angle to 35° in either direction to prevent any possible jackknife. However, such large articulation angles were never attained during testing.

2.2/ Test Site

All tests were conducted at the MTC Research and Development Test Facility at Huron Park, 50 km north of London, Ontario. The driving manoeuvres were performed on a resurfaced section of runway about 200 m long and 50 m wide (with a 400 m run-in) near the north end of a runway about 1000 m in length. The test vehicle always travelled from south to north during test runs, and returned to the start along taxiways and the hanger apron.

The asphalt surface of the test pad had been sealed with an oil emulsion to provide a low skid number and was kept wet at all times by using a sprinkler system supplemented by hoses, maintaining a water depth between 0.3 mm and 10 mm (in occasional pools). This ensured that any loss of control would result in the vehicle sliding rather than rolling over. The watering system was designed so that the vehicle's windshield wipers were not required and the driver's view was unobstructed. The use of a wet surface was consistent with the findings of MTC research personnel that the majority of tractor/semitrailer loss-of-control accidents investigated during the winters of 1979/80 and 1980/81 involved wet or slippery roads.

2.3/ Driving Tasks

The testing area was laid out for the driving tasks as shown in Figure 3. Fifteen poles were set at 20 m intervals along the right-hand side of a 3.66 m wide straight driving lane. This lane was marked by a broken line on the right-hand side and by a solid line on the left-hand side. The solid line was intended to represent the centreline of a two-lane undivided highway. A further 3.66-m wide lane was marked on the other side of the centreline by orange pylons set 20 m apart opposite each pole. An air pressure hose activated switch was placed in the right-hand lane 18.7 m before Pole 1, located so that the vehicle's right-hand wheels passed over it. This switch, when triggered by the vehicle's right front wheel, sent a signal via a radio link to the on-board data acquisition system, uncaging the gyros and initializing the distance counter.

Each pole was mounted in a grey plywood box-like base anchored to a cement patio stone (see Figures 4 and 5). The poles were 4.8-cm diameter black plastic pipes with their tips 3.7 m above ground level. The poles were set back 0.55 m from the lane edge. Orange tape stripes were used to increase pole visibility. One pole, known as the active pole, was pivoted inside its mounting box and could be triggered remotely by a radio link to fall at a predetermined distance in front of the vehicle. This pole was indistinguishable from the others and before each run was placed according to a randomized pattern between pole locations 5 and 11 without the driver's knowledge (unless desired). The active pole is shown as it falls in Figures 4 and 5. When released, it pivots with the aid of a spring mechanism and its tip hits the ground in about 1.4 s, extending 2.73 m into the lane along which the vehicle is being driven.

The driving tasks performed by the test subjects utilized the active pole. In each case, the driver was instructed to approach the test area in the right-hand lane driving in 5th-over gear with the accelerator pedal fully depressed. This ensured that the engine speed was controlled by the governor and that the vehicle speed was maintained very close to 50 km/h. The drivers were instructed to maintain this condition throughout the test manoeuvres unless safety considerations dictated otherwise. The individual driving tasks employed are outlined below.

(i) Short Preview -- The active pole was placed between pole locations 5 and 11, inclusive. The driver was not aware of the active pole location. It was triggered to fall when the vehicle's front bumper was 32.5 m away from it. The driver was required to steer around the fallen pole without hitting it and then return as quickly as possible to his original lane.

(ii) Long Preview -- This was the same as the Short Preview task except that the active pole was triggered at a distance of 52.5 m in front of the vehicle's front bumper.

(iii) Parked Pole -- In this task, the active pole was down and blocking the driving lane throughout the vehicle's approach. The driver was instructed to avoid the pole while minimizing his time spent in the adjacent lane.

(iv) Blank Run -- In this case, the active pole was not triggered and no obstacle avoidance manoeuvre was required. Blank runs were included to increase the uncertainty attached to a pole falling event.

(v) Designated Pole; Short Preview -- This was the same as (i) above, except that the active pole was marked with an orange pylon and the driver was informed of this.

(vi) Designated Pole; Long Preview -- The same as (v) above, but using a preview distance of 52.5 m.

3/ INSTRUMENTATION

The MTC vehicle instrumentation package consists of a 42-channel data acquisition system, a Humphrey Model CF18-0907-1 instrumentation package, and a number of individual sensors. In the present tests, the outputs from seven sensors were recorded and employed in subsequent data analysis. These sensors are described briefly below.

3.1/ Sensors

(i) Steering Wheel Angle (δ_s) -- A pull-cord multi-turn potentiometer (employing a mechanical spring return mechanism) was employed by wrapping its cord around the steering column.

(ii) Yaw Angle (ψ) -- The yaw or vehicle heading angle was generated by the Humphrey instrumentation package mounted in the cab sleeper on the vehicle's centreline (see Figure 6). Its gyro-stabilized platform was uncaged by the air switch located on the roadway before Pole 1. The instrument's erection mechanism was not employed as the test duration was so short (25 s) that no significant gyro drift occurred.

(iii) Lateral Offset (y) -- This measurement employed a Human Factors Research Inc. lane tracker based on a modified video camera using a linear photodiode array at the focal plane. It was located on the cab roof on the vehicle centreline looking forward and down (see Figure 7). This system works by detecting the location of the solid road centreline in the camera's field of view. The details of the relevant geometry are described in Appendix A. A 12.5 mm lens with a polarizing filter was employed giving a roadway lateral scan of ± 2.75 m. The resolution of the system is one part in 256 (or 2.2 cm). The output was corrected for vehicle roll and heading angles using the equations developed in Appendix A. The geometrical parameters specifying the location and attitude of the lane tracker are contained in Table 2.

(iv) Speed (V) -- Vehicle forward speed was obtained from a sidewheel mounted beside the left fuel tank (see Figure 8). This unit consists of a freely-rotating wheel, inflated to 206 kPa (30 psi) with a magnetic pickup placed close to 60 holes drilled in a ring mounted on the wheel.

The passage of the holes past the pickup generates a signal with a frequency proportional to speed.

(v) Distance (s) -- The pulses generated by the sidewheel sensor, of (iv) above, were detected and accumulated to provide a signal proportional to distance travelled. An analog ramp signal was generated which reached full scale after 1000 counts and was then reset to zero. Each full ramp corresponded to a distance of 21.3 m.

(vi) Roll angle (ϕ) -- The tractor's roll angle relative to the local vertical was provided by the Humphrey instrumentation package following the description of (ii) above.

(vii) Pole Trigger -- When a triggering signal was transmitted to the active pole, this event was recorded as a non-zero signal level on one of the data acquisition tracks. The active pole electronics were set up to release the pole 0.54 s following this trigger signal. This system is fully described in Appendix B.

3.2/ Data Acquisition System (DAS)

The data acquisition system consisted of a constant bandwidth, frequency modulated, multiplexing system mounted in the sleeper portion of the test tractor. This system provided the necessary transducer excitation and signal conditioning to permit multiplexing and recording of up to 42 individual signals. A precision time code produced by a crystal-controlled clock was also recorded for data synchronization during data playback. Figure 9 shows the major components of the data acquisition system.

Electrical signals produced by the transducers were conditioned by individual plug-in type adapter cards within the Metraplex Model 300 FM multiplexing unit. Figure 6 shows the unit in the tractor and the DAS control panel. A predetermined maximum input stimulus to the transducer was selected and the conditioner parameters adjusted to provide an output signal of ± 0.5 V for the chosen ± Full Scale input. Each conditioned output signal was then applied to a voltage-controlled oscillator (VCO), the outputs of which, when summed, performed the multiplexing operation.

The VCOs were arranged in groups of seven having centre frequencies 2.0, 4.0, 6.0, 8.0, 10.0, 12.0, and 14.0 kHz and peak deviations of 500 Hz for Full Scale inputs. In addition to the data channels, each multiplex contained a 24.0 kHz precision frequency from a crystal-controlled oscillator and an Autoset Command signal on a 16.0 kHz channel. Hence, each multiplex contained seven data channels plus calibrate command and tape speed compensation data. These signals were sent via a telemetry link to a Honeywell 5600C tape recorder located in the test facility laboratory and were recorded on separate tracks. The data channels were monitored, and one track was played back through a chart recorder in real time.

Upon completion of testing each day, data stored on the magnetic tape were replayed one track at a time along with the precision time code from track number 4. Data channels were demultiplexed by a set of FM discriminators tuned to the same centre frequencies generated by the voltage-controlled oscillators during the recording period. In this way, each discriminator voltage output was a reproduction of the conditioned transducer signal applied to the individual VCO.

The data bandwidth of these output signals was controlled by a set of plug-in output filters on the discriminators. Typically, 3 Hz 5-pole linear phase filters were used for "quick-look" records, and 50 Hz 5-pole linear phase filters were used when data were replayed for digitizing. With a peak deviation of 500 Hz, data bandwidths up to 100 Hz could be recovered with a deviation ratio of 5 which reproduces the input data with less than 1% distortion.

A major source of error in all FM multiplexing systems using tape recorders is small variations in the reproduced frequencies due to similar variations in tape speed (wow and flutter). These variations are superimposed on the data and appear as fluctuations in the reproduced signal. To compensate for this, the precision crystal-controlled frequency which was summed with the data multiplex was reproduced using a separate discriminator. Any variations in this output were due to tape speed variations and, when coupled with the data discriminators, this subtracts to a large extent the source of error. Therefore, each resultant output signal was a faithful reproduction of the transducer output.

To ensure proper calibration of the data discriminators, the autoset zero command signal was introduced at regular intervals (twice a day) throughout the test period. This command, when present, automatically instructed all data discriminators to drive to zero volts at the output, thus compensating for drift in the centre frequency of the individual VCOs. In addition, an autoset span command was also introduced, when an "on playback" command automatically adjusted the discriminator output to the desired full scale value. By using the autoset command functions, the complete data acquisition system was calibrated to an accuracy of ±1.25% of Full Scale.

A calibration sequence was recorded before each run.

3.3/ Data Handling

At the completion of testing each day, one (or more) FM tape(s) contained a record of every run. Test records included the allocation of sensors to each track and channel on a daily basis. Calibrations were obtained for every sensor relating the magnitude of the sensed variable to the DAS output to this tape.

The FM tapes were processed using these calibrations to provide a time history of every variable of interest for every run required for analysis. Data tracks of interest were passed through 50 Hz low-pass analog filters and then digitized by a 12-bit A/D converter controlled by a PDP-8/A minicomputer. A timing interface was fed the section "start" and "stop" times and switched the A/D converter "on" and "off" as the time code on the FM tape reached these times. At the same time, low-speed oscillograph records were produced for each track digitized.

The minicomputer produced a digital tape containing the test data sampled 100 times per second for each channel. The data were in "counts", where 1 count = 1.221 mV and full scale was -819.2 to 819.2 counts. These raw data were not ordered properly for further data reduction so they were processed on the MTC IBM 370-series computer to sort and check them for errors. This process used program AVRAW(4), which produced a second digital raw data tape.

The tape was then used to generate time histories of the variables of interest using the programs AVENG(5) and AVCAL(6). The raw run data were corrected for instrumentation drifts using the immediately preceding calibration, and then filtered with a non-recursive low-pass 3 Hz digital filter. The data were then converted into engineering units using the sensor calibrations previously stored in a computer data set. Both linear and nonlinear calibrations were used.

These run data, suitably labelled and stored on magnetic tape, were then available for further analysis as required, such as plots or as input to analytical computer programs.

The data are naturally subject to errors from several sources, such as sensor, calibration, data acquisition system and reduction errors. Overall errors were estimated to vary between 1.0% and 2.5% of full scale output.

In the case of the lane tracker output signal, which was combined with vehicle heading angle (ψ) and roll angle (ϕ) to generate the distance of the tractor's centre of gravity from the roadway centre stripe (see Appendix A), an additional correction was required because the road surface was not perfectly level. Figure 10 gives sample plots of the tractor roll angle relative to the vertical for two cases as a function of distance travelled from Pole 1.

The one case represents a Blank Run with no obstacle avoidance manoeuvre and thus the recorded values of ϕ represent the lateral slope of the road. The second case was a Short Preview Run and thus represents the most severe manoeuvres employed.

The roll angles for this latter case represent the sum of roadway slope and tractor sway due to the manoeuvre. Since the roll angle employed in Appendix A should actually be referenced to the local vertical to the road surface, the roll gyro output during the manoeuvres was corrected by subtracting from it the local road slope. This corrected value of ϕ was then employed in generating the centre of gravity's location relative to the centre stripe.

4/ DRIVER MODEL

The driver model for the obstacle avoidance manoeuvre is fully described in References 1 and 2; thus, only a brief outline will be given in this section. The dynamic characteristics of this linear model are represented by the transfer function:

$$\frac{\bar{\delta}_s}{\bar{\psi}_t} = G_\psi e^{-\tau s} \frac{T_L.s + 1}{R_I.s + 1} \qquad (1)$$

Here ψ_t is the sight point angle, defined to be the angle between the centreline of the vehicle and the driver's line of sight (see Figure 11). In this model, it is assumed that either a specific point or a point a fixed distance ahead of the driver is the point of visual fixation during each of several model phases. It was found that, in general, a minimum of three driver model phases were required.

Phase I -- This phase begins once the falling pole is detected (as indicated by the initiation of a large steering wheel response).

Phase II -- This phase begins once the vehicle is established on a trajectory which will clear the end of the obstacle pole (as indicated by $\psi_t = 0$).

Phase III -- This phase begins when the vehicle is a specified short distance from the obstacle pole and ends once the vehicle is again established in the right-hand lane.

During Phase I, the sight point is taken to be a point y_o metres to the left of the end of the obstacle's final position. During Phase II, the driver's sight point is assumed to be the centre of the left-hand lane at a fixed distance ahead of the vehicle. During Phase III, the sight point is taken as the centre of the right-hand lane at a fixed distance ahead of the vehicle.

5/ EXPERIMENTAL DETAILS

5.1/ Subjects

Four test drivers participated, all of whom were truck operators employed by the MTC with Ontario Class "A" licences. Some details concerning these drivers are listed in Table 3. Drivers 1, 3 and 4 normally operated a conventional two-axle tractor pulling a single-axle float or a low-bed trailer with a 10.7 m bed. Driver 2 primarily drove the cab-over-engine test tractor, with one or two trailers, during bridge testing and vehicle dynamics research. Thus, he was more familiar with the vehicle and the most experienced test driver of the group. The drivers received their normal MTC salary during testing, with no bonus payments related to the project.

5.2/ Training

Initial training was designed to familiarize the driver with the test vehicle. It consisted of normal driving around the test track, accelerating through the gears, and mild manoeuvring. This phase took between 2 and 8 h per driver.

The next training phase involved single- and double-lane change manoeuvres on the wetted testing area using a course laid out with orange marker pylons. These represented moderate to severe manoeuvres and testing lasted from 3 to 4 h per driver.

Following the above general training period, practice with the falling obstacle pole was started. During these runs, the position of the active pole was selected at random from pole locations 5 through 11. This began with two runs using the Long Preview distance (52.5 m). The drivers were first given the instructions labelled C.1 in Appendix C. These trials were designed to see how the drivers would react if they were not specifically told to avoid using the brakes during the manoeuvre. This was followed by a series of training runs at a constant forward speed of 50 km/h. The instructions employed are labelled C.2 and C.3 in Appendix C. Instruction C.2 was only used during the initial trial of this sequence. Before each of these trials the drivers were told which

event would take place. The series of training runs employed consisted of (in order):

- 12 runs -- Long Preview (52.5 m)
- 6 runs -- Designated Pole, alternating Long and Short Preview
- 12 runs -- Short Preview (32.5 m)
- 6 runs -- Parked Pole

This phase of the training took about 3 to 4 h per driver.

5.3/ Production Runs

Production runs began once training was completed and the drivers were producing consistent results. A randomized ordering of the following tasks was employed (also with randomized active pole assignment among locations 5 through 11):

- 8 runs -- Short Preview (32.5 m)
- 8 runs -- Long Preview (52.5 m)
- 8 runs -- Blank Run
- 8 runs -- Parked Pole
- 4 runs -- Designated Pole, Short Preview
- 4 runs -- Designated Pole, Long Preview

The drivers were not told whether to expect a Long or Short Preview case or a Blank Run on any individual trial. In the case of the Parked Pole or the Designated Pole, of course, the driver was aware of the location of the obstacle well in advance of his manoeuvre. Production runs were completed during two 3-h sessions per driver.

5.4/ General Procedures

During all phases of this study, an experimenter rode in the truck cab with the test driver. A test engineer operated the data recording instruments located at the test facility laboratory. Up to four other assistants looked after running the track water sprinkler system and moving the active pole to its assigned location for each test run. The moving of the active pole was accomplished during a period of time when the driver could not see the testing area. Testing took place during the summer of 1981 under generally sunny conditions.

6/ DATA ANALYSIS

6.1/ Driver Model Fitting Technique

The driver model fitting techique and its associated computer code are described in Reference 2. A brief outline of the method is presented in this section. The model takes the form:

$$\dot{\underline{x}}(t) = \underline{A}\,\underline{x}(t) + \underline{B}\,\underline{u}(t) \tag{2}$$

$$\underline{y}(t) = \underline{x}(t) + \underline{b} \tag{3}$$

where $\underline{x}(t)$ is the system state vector, $\underline{u}(t)$ is the control or input vector and $\underline{y}(t)$ is the calculated response variable. The vector $\underline{b}$ represents any constant offsets present in the system. If $\underline{z}(t)$ is the experimentally measured driver/vehicle response to the input $\underline{u}(t)$, then it is desirable to choose $\underline{A}$, $\underline{B}$ and $\underline{b}$ so as to obtain a good match between $\underline{y}(t)$ and $\underline{z}(t)$.

The present algorithm achieves this matching by minimizing the quadratic cost functional:

$$J = \frac{1}{T}\int_0^T (\underline{z}-\underline{y})^T \underline{D}\,(\underline{z}-\underline{y})dt \tag{4}$$

where T is the record length of the experimentally measured data file and $\underline{D}$ is a positive definite symmetric weighting matrix.

Now let $\underline{c}$ be a column matrix made up from all of the model's free parameters, i.e., the elements of $\underline{A}$, $\underline{B}$ and $\underline{b}$. The gradient of J with respect to the elements of $\underline{c}$ is:

$$\Delta_c J = \left(\frac{\partial J}{\partial c_1}, \frac{\partial J}{\partial c_2}, \ldots \frac{\partial J}{\partial c_N}\right)^T \tag{5}$$

As the elements of $\underline{c}$ are varied, the minimum in J occurs when:

$$\Delta_c J = \underline{0} \tag{6}$$

A modified Newton-Raphson algorithm searches for this minimum by first expanding $\Delta_c J$ in an approximation to a truncated Taylor's series. It then seeks that increment in model parameter space which produces $\Delta_c J = \underline{0}$ in a single step as predicted by this approximate expression. Because of the approximations involved, this generates a new set of parameters $\underline{c}$ which does not exactly produce the desired minimum in J. Thus, further iterations must be carried out until a suitably small value for J is obtained.

In order to render the driver model represented by Equation 1 compatible with the fitted model form of Equation 2, we must explicitly remove the pure time delay term $e^{-\tau s}$ from the driver model. This is done by considering a model relating a time-advanced steering wheel response ($\delta_{s\tau}$) to the sight point angle input signal. The model form for the driver then becomes:

$$\frac{\bar{\delta}_{s\tau}}{\bar{\psi}t} = G_{\psi} \frac{T_L.s + 1}{T_1.s + 1} \tag{7}$$

In the time domain this becomes:

$$\dot{\delta}_{s\tau}(t) = \frac{-\delta_{s\tau}(t)}{T_I} + \frac{1}{T_I} \{G_{\psi}\psi_t(t)\} + \frac{T_L}{T_I} \{G_{\psi}\dot{\psi}_t(t)\} \tag{8}$$

or $$\dot{\underline{x}}(t) = \underline{A}\, \underline{x}(t) + \underline{B}\, \underline{u}(t) \tag{9}$$

where $$\underline{x}(t) = \delta_{s\tau}(t) \tag{10}$$

$$\underline{u}(t) = [\psi_t(t),\ \dot{\psi}_t(t)]^T \tag{11}$$

$$\underline{A} = -\frac{1}{T_I} \tag{6.11}$$

$$\underline{B} = \left[\frac{G_\psi}{T_I}, \frac{T_L G_\psi}{T_I}\right]$$

$$T_I = -1/A_{11}$$

$$G_\psi = -B_{11}/A_{11}$$

$$T_L = B_{12}/B_{11}$$

The experimentally measured values for $\underline{z}(t)$ and $\underline{u}(t)$ are required in order to apply this technique. In this instance $\underline{z}(t)$ (or $\delta_{s\tau}$) is produced by time-advancing the measured steering wheel response $\delta_s(t)$ by τ seconds. The value of τ must be selected a priori and the best value of τ determined by observing how J varies with τ.

6.2/ Input Data Files

The data tapes described in Section 3.3 were further processed to generate the input data files required by the driver model fitting algorithm. In order to lower the data analysis costs, only every fifth sample was used -- thereby reducing the effective data sampling rate to 20 Hz. At this stage, only the following variables were required: s, y, δ_s, ψ. The s file was further smoothed by performing a running average over five adjacent data samples in order to reduce instrumentation noise. The variables s and ψ were then combined to generate x, the distance along the road at which the tractor's centre of gravity is located. Using the information provided by the output of the air switch and the time at which the pole trigger signal was transmitted, the location of the active pole was established and x shifted to equal zero when the tractor's centre of gravity reached the active pole location. Only data corresponding to $-90\ m < x < 80\ m$ were retained.

When it is desired to average together the results obtained from several runs, it is apparent that this is best accomplished by averaging data corresponding to the same value of x (as generated above). In order to perform this operation, it is first necessary to generate data files for equally spaced values of x. This was accomplished by applying linear interpolation. This resulted in the following variables being generated at equally spaced values of x: t, y, δ_s, ψ. The desired averaging was then carried out on the latter four variables. Because the model fitting algorithm operates in the time domain it is then necessary to further process the data to generate data files equally spaced in time. Again this was carried out employing linear interpolation to produce data spaced at 50 ms intervals for x, y, δ_s and ψ.

As seen from Equations 10 and 11, the model fitting algorithm requires data files of $\delta_{s\tau}$, ψ_t and $\dot{\psi}_t$ equally spaced in time for each driver model phase. $\delta_{s\tau}$ was generated by time-advancing δ_s by τ seconds relative to ψ_t and $\dot{\psi}_t$ in the data files.

In computing ψ_t, the location of the driver's eyes was assumed to be on the centre line of the tractor at a point the same distance ahead of the centre of gravity as the driver himself. This simplifying assumption ensures that $\psi_t = 0$ corresponds in the steady state to the vehicle heading directly towards the chosen sight point.

$\dot{\psi}_t$ was generated for each model phase by using the approximation

$$\dot{\psi}_{tk} = \frac{\psi_{t(k+1)} - \psi_{t(k-1)}}{2\Delta t} \qquad (13)$$

where $$\psi_{tk} = \psi_t(k\,\Delta t) \qquad (14)$$

and Δt is the sampling interval. The initial and final values for a model phase were obtained from a linear extrapolation on $\dot{\psi}_t$. It should be noted that the ψ_t for each phase was treated as an independent data

set. The step changes in ψ_t which occur at the beginning of each phase were retained but the corresponding Dirac delta function in $\dot{\psi}_t$ at these locations were removed as model inputs because it was reasoned that human drivers would not attempt to respond to such spikes (as was verified by the model fitting results).

7/ DISCUSSION OF RESULTS

The processed experimental measurements were stored in digital data files for use in the driver model fitting process. Typical single production run records of steering wheel angle, heading angle, lateral offset, and roll angle are shown in Figures 12, 13, 20 and 21. In these and subsequent plots, the distance (short for distance travelled s) is referenced to the location of the obstacle pole. The small gaps in the data plotted in Figures 15 to 37 indicate the location of the interfaces between the various model phases. It can be seen that the roll angle gyro output signal was fairly noisy. The general features of these records are quite similar to those reported in Reference 1 for obstacle avoidance manoeuvres performed in a fixed-base driving simulator. As expected, the Short Preview tasks generated the largest peak values for system variables. An accelerometer located in the tractor indicated typical peak lateral accelerations of 0.25 g for Long Preview and 0.30 g for Short Preview tests.

Following an inspection of the complete set of data plots, it was discovered that although no runs had been lost due to equipment failure, a few had to be discarded because the drivers did not follow their instructions. In particular, Subjects 2 and 4 each began three of their four obstacle avoidance manoeuvre lane changes for the Designated Pole, Short Preview case, before the pole was triggered to fall. These production runs were therefore dropped from the final analysis.

7.1/ Training Effects

For the first two runs during which each driver was faced with a falling pole, they were not given any instructions concerning the use of the brakes. In all cases they carried out the obstacle avoidance manoeuvre without applying any braking. This is consistent with the correct driving technique for avoiding a jackknife accident on wet pavement.

In order to assess the effect of practice on the drivers' performance in the obstacle avoidance manoeuvre, their first two training runs (as described above) and their last two production runs (all for Long Preview) were compared. Two parameters were employed: their reaction time

from when the pole began to fall until a steering wheel response was detected (τ_R), and the time that the centre of gravity of the tractor spent in the passing lane (Δt_1). Because Subject 2 had participated in some preliminary set-up trials he could not be used in this comparison. The results are presented in Figure 14. No conclusive trends were observed. In the case of τ_R it was found that two subjects reduced their reaction time with training while the other subject increased his. All subjects tended to reduce their dwell-time in the passing lane with training. Tests with a larger population of drivers are required before drawing any conclusions about training effects on this manoeuvre.

7.2/ The Model Fitting Process

The first step in the model fitting process is to specify the driver's sight point for each phase of the manoeuvre. Because eye-tracking measurements were not taken during the present tests it was decided to use the values for Phases II and III employed in Reference 2 for simulator-derived data. Thus, during Phase II the sight point was taken to be the centre of the passing lane 40 m ahead of the driver, and during Phase III it was taken to be the centre of the right-hand lane 20 m ahead of the driver.

For Phase 1, the driver's sight point was taken to be a fixed point on the roadway to the left of the tip of the fallen obstacle pole. This distance y_0 (see Figure 11) was assumed equal to the distance of the tractor's centre of gravity from the tip of the pole at the moment of passage. The average value for each subject was employed in analyzing all his runs. The values of y_0 are to be found in Table 4. It is seen that the values of y_0 tend to be greater for Long Preview than for Short and greater for Designated than for unspecified pole runs. The values for the Parked Pole runs tended to be similar to those for the Designated Long. The grand average results in Table 4 (averaged over all four subjects) were used in analyzing the grand average driver data files.

The next step is to identify the beginning and end of each phase of the manoeuvre for each run to be analyzed. In the case of Long Preview (52.5 m), the manoeuvre is divided into three phases. The start of the Phase I steering response is taken to be the point where the large

steering wheel pulse begins following the triggering of the obstacle pole. Due to the time delay τ within the driver, the start of the Phase I ψ_t input is assumed to occur τ seconds before δ_s. The end of the Phase I model input and the beginning of the Phase II model input occurs when ψ_t first goes to zero. The end of the Phase I model output occurs τ seconds later. The end of the Phase II model input and the start of the Phase III model input occurs when the driver's eyes are 4 m from the obstacle. The end of Phase II occurs τ seconds later. The end of the Phase III model input occurs when the driver's eyes are 80 m past the obstacle and the end of the Phase III model output occurs τ seconds later. Thus, it is seen that the section of recorded δ_s assigned to each of the three phases changes with the value of τ employed.

In the case of the Short Preview distance (32.5 m), it was found that the Phase II segment was so short that it was not possible to fit a separate model form to it. The solution was to combine Phases I and II together into a phase designated I + II which begins in the same manner as Phase I, ends in the same manner as Phase II, and employs the same sight point as Phase I.

Once a value is assigned to τ, the time delay, the data files of ψ_t and $\dot{\psi}_t$ can be generated for each run. To be consistent, it was necessary to employ the same values of τ for all model phases. This prevents gaps and overlaps at the interfaces between the model phases. All other model parameters were free to vary from phase to phase. The value of τ had to be selected before applying the model fitting algorithm with the model of Equation 8. The best value for τ was determined by examining its influence on the fit parameter J for a given set of experimental data. A value of J was generated for each model phase. For the purposes of selecting τ, the sum of the individual J's was employed (denoted J_2 or J_3). A minimum in J_2 was sought for the Short Preview cases and in J_3 for the Long. Typical plots of ψ_t and $\dot{\psi}_t$ are contained in Figures 15 to 18.

The model fitting algorithm search for values of A_{11}, B_{11}, B_{12} (see Equation 12) and b (a scalar bias term) for each model phase. It was found that good fits to Phases I and I + II could be achieved with b set identically to zero. (Note that in the present analysis $\underline{b}$ is a scalar.) The

cases with nonzero values for b can be considered to have a visual sight point located further to the right than was originally assumed by a distance to the right given by:

$$\Delta S = \frac{\ell . b}{57.3 G_{\psi}} \quad (m)$$

where b is in degrees and ℓ = 40 m for Phase II and ℓ = 20 m for Phase III. In computing the value of the cost functional J, the matrix $\underline{D}$ in Equation 4 was 1 x 1 and its value taken to be unity. Thus, J represents the mean square of the difference between the driver model and the actual driver's steering wheel angle response.

Model fits were performed on single run data, averaged run data, and grand average run data. The averaged run data for each subject were produced by averaging together all his production run data files (as outlined in Section 6.2). The number of production runs for each driving task is reported in Section 5.3. In the case of the Designated Pole Short Preview task, Subjects 2 and 4 only produced one acceptable run each, due to premature steering responses. The grand average run files were generated by averaging together all the production runs of all four subjects for each task.

In general (with a few exceptions), the model fitting algorithm converged smoothly to a final solution in less than six iterations. Each model phase was fitted as a separate operation.

As indicated above, the time delay parameter τ had to be specified before running the model fitting algorithm and the best value selected by observing its effect on J. Figure 19 shows the variation of J with τ for the three phases of the grand average run for the Long Preview case. It can be seen that J_3 has a definite minimum near τ = 0.2 s. The variation of the model parameters with τ is similar to that reported in Reference 2 for driving simulator derived data. (Note that $T_L \equiv 0$ was found to produce the best results for Phase II.)

The results of applying the model fitting algorithm to the present experimental data are presented in Tables 5 to 9 and in Figures 20 to 34. It is seen that there is a general improvement in the model fit (J) as more data are averaged together before carrying out the model fitting process. This occurs because the averaging process removes the low-amplitude random dither present on the individual runs which the driver model is not capable of generating. Fits to Long Preview runs are better than those to Short Preview runs (the Parked Pole run appears similar to the Long Preview run in this respect). Fits to the Designated Pole runs are poorer than those to the corresponding randomly-selected pole runs. In general, quite acceptable fits to all runs were achieved, as can be seen by inspecting Figures 20 to 34.

In the fitting process, it was found that the best results were achieved with $T_L \equiv 0$ for Phase II of all tasks using the Long Preview distance (including the Parked Pole runs). Also, a minimum τ value of 0.1 s was imposed on the model fits. It was found that the model fitting process was quite sensitive to slight changes in the driver's steering response patterns, as can be seen from the variability in the model parameters reported in the tables. The sensitivity of the fitting process to individual parameter variations was checked by using the average Long Preview run of Subject 3. The results are recorded in Table 10. For each model phase, the best-fit parameter set serves as the reference case (data enclosed in the boxes in the table). First, the time delay τ was changed by 0.1 s and the fitting process applied to generate a new set of parameters. The percent change in J (ΔJ%) normalized by the percent change in τ (Δ%) is recorded. Next, the reference set of model parameters are again selected with only one of them changed by 20% (as indicated by the underscore). The resulting normalized change in J is recorded. It is seen that the results are least sensitive to changes in τ and sight point distance (and to ΔS in Phase III). Other parameter variations produced a significantly greater increase in J.

In achieving the best fit, it is seen from Tables 5 to 9 that negative parameter values are quite common. The Bode plots of Figure 35 show how one combination of negative parameters (Phase I, Long Preview) influences the driver model's amplitude and phase characteristics. In addition,

most values of ΔS for Phase II are too large to be interpreted as slight modifications to the sight point. In these instances, this parameter must be considered as a key model feature representing a specific offset in the steering wheel response generation process and, as such, must be treated as an additional model element.

Once driver models based on averaged run and grand average data have been generated, it is of interest to see how well they predict the steering wheel response for individual runs. To illustrate this process, the results from a single Short Preview run of Subject 3 have been modelled using his averaged run and grand average model. The results are presented in Figures 36 and 37. Although the general features of the steering wheel response are represented, it can be seen that the Phase III segment fit is somewhat marginal. The actual impact of these differences would have to be studied using a closed-loop system simulation.

8/ SUMMARY

A series of tasks involving the obstacle avoidance manoeuvre has been carried out by four driver subjects. These field trials employed an instrumented White Freightliner tractor/semitrailer truck. The performance of the drivers has been studied and linear driver models fitted to their steering wheel responses by using a modified Newton-Raphson technique. The following is a summary of the findings of the present project.

1/ Insufficient data were generated to allow conclusive results regarding training effects. Two out of three drivers reduced their reaction times in responding to the falling pole with training. All subject drivers tended to reduce their dwell-time in the passing lane with training.

2/ The present driver model successfully fitted almost all of the experimental records.

3/ Generally better model fits were achieved as more data were averaged together.

4/ Better driver model fits were achieved for runs employing the Long Preview distance.

5/ In Phase II of the model, a constant steering wheel offset must be incorporated in order to achieve good fits to the experimental data.

REFERENCES

[1] Reid, L.D., Graf, W.O. and Billing, A.M., "A Preliminary Simulator Study of the Obstacle Avoidance Manoeuvre," Ontario Ministry of Transportation and Communications, CVOS-TR-80-07, May 1980.

[2] Reid, L.D., Graf, W.O., Billing, A.M. and Solowka, E.N., "Fitting of Linear Driver Models to Simulator Derived Data," Ontario Ministry of Transportation and Communications, TVS-CV-81-111 and University of Toronto, UTIAS Rept. No. 255, June 1981.

[3] Etkin, B., Dynamics of Atmospheric Flight, John Wiley & Sons, New York, 1972.

[4] Glowacki, H. and English, A., "Articulated Vehicle Test Data: AVRAW," Ontario Ministry of Transportation and Communications, Engineering and Management Systems Branch, October 1976.

[5] English, A., "Articulated Vehicle Test Data: AVENG," Ontario Ministry of Transportation and Communications, Engineering and Management Systems Branch, July 1977.

[6] Billing, A.M., "Computer Program AVCAL: Channel Configuration and Calibration Maintenance," Ontario Ministry of Transportation and Communications, Research and Development Branch Report CVOS-TR-79-05, May 1979.

Table 1/ Vehicle Specification

TRACTOR

Model:	White Freightliner with tandem drive axles, 4.45 m wheelbase, COE (sleeper type)		
Engine:	V-12 Detroit Diesel, 465 hp @ 2100 rpm		
Steering:	37.6:1 constant ratio, power assist		
Axles:		Front	Rear
	Capacity	8165 kg	19 960 kg
	Suspension	Leaf spring	Hendrickson RTE-440 1.83 m spread walking beam
	Static load (bobtail)	4530 kg	4800 kg
Tires:	Firestone Transport I		
	Type	Bias ply rib type, load range F	
	Size	11.00 - 22.5	
	Pressure	586 kPa (85 psi) front axle; 517 kPa (75 psi) drive axles	
Wheelbase:	4.45 m		
Mass centre:	2.29 m aft of front axle 0.91 m above ground		

TRAILER

Model:	King 42 SW "Trombone" flatbed type semitrailer, tandem axles		
Overall length:	7.14 m (min) to 9.58 m (max, test length)		
Axles:	Rating	18 140 kg total	
	Suspension	Reyco tandem model 22B-2-22-W-15-1-49 leaf spring, 1.24 m spread	
Tires:	Firestone Transport I		
	Type	Bias ply rib type, load range F	
	Size	10.00 - 20	
	Pressure	517 kPa (75 psi)	
Wheelbase:	7.60 m		
Mass:		Empty	Loaded
		6690 kg	14 400 kg
Mass centre:	Aft of kingpin	5.16 m	4.73 m
	Above ground	1.16 m	1.58 m

Table 2/ Lane Tracker Mounting Parameters

x_d	2.74 m
y_d	0
z_d	-2.57 m
z_b	-0.60 m
z_{cg}	-0.20 m
θ_i	-29.6°

Table 3/ Test Subjects

	Subject			
	1	2	3	4
Age (years):	49	48	44	54
Glasses worn:	No	No	No	Yes
Years driving:	30	27	29	38
Years driving trucks:	15	27	20	33
km/year (all vehicles):	48 000	30 000	24 000	68 000
km/year (heavy trucks):	24 000	4 000	8 000	40 000

Table 4/ y_o(m) Based on Averaged Runs

SUBJECT	LONG	SHORT	DESIGNATED LONG	DESIGNATED SHORT	PARKED
1	2.08	1.65	2.23	1.95	2.06
2	1.81	1.65	1.78	1.95	1.66
3	1.92	1.62	1.82	1.72	1.73
4	1.95	1.39	2.06	1.91	1.93
GRAND AVERAGE	1.94	1.58	1.98	1.88	1.98

Table 5/ Best-Fit Driver Model Parameters, Long Preview

Subject No.	Run No.	Phase	τ (s)	T_I (s)	T_L (s)	G_ψ	ΔS (m)	J $(deg)^2$	J $(deg^3)^2$
3	5	I	0.1	-0.82	1.35	-30.20	-	2.47	86.72
		II	0.1	2.08	0	45.14	4.26	28.46	
		III	0.1	0.30	0.23	26.39	0.03	55.79	
3	6	I	0.1	4.54	0.36	304.60	-	1.76	114.10
		II	0.1	1.36	0	40.87	2.60	11.79	
		III	0.1	0.09	-0.14	21.06	-0.01	100.5	
3	7	I	0.2	-1.30	1.60	-35.95	-	3.42	21.87
		II	0.2	1.20	0	1.92	183.10	0.93	
		III	0.2	0.81	0.71	27.64	0.06	17.52	
3	8	1	0.1	-0.76	2.21	-20.23	-	3.07	21.52
		II	0.1	1.30	0	43.86	3.42	0.09	
		III	0.1	0.11	-0.07	20.88	-0.10	41.46	
1	AVERAGE	I	0.3	-0.24	2.16	-47.43	-	0.53	13.93
		II	0.3	5.06	0	-166.30	-3.92	0.07	
		III	0.3	0.93	1.04	18.82	0.12	13.33	
2	AVERAGE	I	0.2	0.83	0.20	59.18	-	1.09	13.37
		II	0.2	1.05	0	4.69	19.90	2.23	
		III	0.2	1.21	0.95	30.08	-0.08	10.05	
3	AVERAGE	I	0.1	-0.63	2.58	-11.56	-	1.45	14.53
		II	0.1	1.89	0	44.16	4.10	2.09	
		III	0.1	0.53	0.40	29.75	0.04	10.99	
4	AVERAGE	I	0.2	1.95	0.74	81.71	-	8.39	29.53
		II	0.2	-5.21	0	19.79	-25.70	2.22	
		III	0.2	0.41	0.37	26.03	0.13	18.92	
GRAND	AVERAGE	I	0.2	-0.82	3.17	-12.01	-	2.60	6.70
		II	0.2	1.83	0	13.56	12.11	0.19	
		III	0.2	0.77	0.74	26.07	0.05	3.91	

Table 6/ Best-Fit Driver Model Parameters, Short Preview

Subject No.	Run No.	Phase	τ (s)	T_I (s)	T_L (s)	G_ψ	ΔS (m)	J $(deg)^2$	J_2 $(deg)^2$
3	5	I + II	0.2	1.36	0.87	84.63	-	38.68	92.92
		III	0.2	0.95	0.80	24.62	0.31	54.24	
3	6	I + II	0.2	1.66	0.91	103.20	-	32.73	122.50
		III	0.2	0.54	0.57	25.92	-0.03	89.74	
3	7	I + II	0.2	1.55	0.99	101.60	-	26.66	98.94
		III	0.2	0.86	0.72	23.71	0.20	72.28	
3	8	I + II	0.2	5.23	1.38	236.80	-	193.10	336.60
		III	0.2	0.54	0.42	30.24	0.21	143.50	
1	AVERAGE	I + II	0.2	1.23	0.84	74.08	-	46.43	57.92
		III	0.2	2.99	2.16	30.59	0.27	11.49	
2	AVERAGE	I + II	0.1	0.83	0.37	81.60	-	50.83	57.19
		III	0.1	0.87	0.69	31.70	-0.33	6.36	
3	AVERAGE	I + II	0.2	2.77	1.16	142.00	-	10.48	36.61
		III	0.2	0.86	0.73	28.48	0.12	26.13	
4	AVERAGE	I + II	0.1	-1.26	1.83	-40.60	-	15.59	39.41
		III	0.1	0.95	0.69	35.72	0.12	23.82	
GRAND	AVERAGE	I + II	0.2	3.33	1.11	161.60	-	14.16	22.37
		III	0.2	1.08	0.98	28.00	-0.03	8.21	

Table 7/ Best-Fit Driver Model Parameters, Designated Pole; Long Preview

	Subject No.	Run No.	Phase	τ (s)	T_I (s)	T_L (s)	G_ψ	ΔS (m)	J $(deg)^2$	J_3 $(deg^3)^2$
**	3	5	I	0.3	0.55	0.42	49.94	-	25.32	91.28
			II	0.3	2.76	0	76.95	2.93	10.53	
			III	0.3	0.57	0.54	30.54	-0.18	55.43	
	3	6	I	0.1	-10.50	0.39	-483.50	-	3.55	84.59
			II	0.1	2.38	0	-8.76	-35.62	18.53	
			III	0.1	0.45	0.30	27.91	0.17	62.51	
**	3	7	I	0.3	-1.59	2.62	-32.01	-	6.19	29.15
			II	0.3	1.65	0	9.02	16.99	5.03	
			III	0.3	10.88	4.15	53.74	0.96	17.93	
	3	8	I	0.1	-1.36	1.49	-39.94	-	4.68	128.5
			II	0.1	3.24	0	-90.35	1625.50	0.37	
			III	0.1	0.45	0.23	26.34	-0.03	123.40	
	1	AVERAGE	I	0.4	11.60	20.72	22.08	-	2.83	20.80
			II	0.4	0.23	0	30.11	-0.55	1.27	
			III	0.4	0.83	1.21	16.09	0.36	16.70	
	2	AVERAGE	I	0.1	-1.20	0.75	-83.55	-	3.29	47.29
			II	0.1	0.99	0	-14.05	-9.11	3.90	
			III	0.1	1.15	0.74	33.51	0.01	40.10	
	3	AVERAGE	I	0.1	-0.26	-8.92	2.54	-	3.33	37.07
			II	0.1	6.10	0	146.60	3.14	0.52	
			III	0.1	0.82	0.59	34.61	-0.04	33.22	
	4	AVERAGE	I	0.3	-0.74	6.01	-6.24	-	6.61	48.8[9]
			II	0.3	-9.77	0	146.80	-8.38	0.99	
			III	0.3	0.36	0.40	26.06	0.15	41.29	
GRAND		AVERAGE	I	0.4	0.72	0.45	32.13	-	4.43	13.34
			II	0.4	1.50	0	34.90	2.84	1.27	
			III	0.4	0.60	0.83	20.74	0.02	7.64	

** Algorithm would not converge for $\tau = 0.1$, $\tau = 0.2$, thus $\tau = 0.3$ was used.

Table 8/ Best-Fit Driver Model Parameters, Designated Pole; Short Preview

Subject No.	Run No.	Phase	τ (s)	T_I (s)	T_L (s)	G_ψ	ΔS (m)	J $(deg)^2$	J $(deg^3)^2$
3	5	I + II	0.2	1.33	0.68	97.66	-	33.07	86.29
		III	0.2	0.53	0.51	27.86	-0.01	53.22	
3	6	I + II	0.1	-2.12	1.12	-108.90	-	9.34	110.70
		III	0.1	0.50	0.33	31.67	0.08	101.37	
3	7	I + II	0.2	2.14	0.95	1.21	-	105.80	232.00
		III	0.2	0.49	0.65	23.08	0.03	126.20	
3	8	I + II	0.2	1.70	0.81	117.00	-	21.97	68.13
		III	0.2	0.19	0.26	24.89	0.08	46.16	
1	AVERAGE	I + II	0.2	1.61	1.01	81.51	-	34.56	82.96
		III	0.2	2.74	1.92	32.42	0.40	48.40	
* 2	AVERAGE	I + II	0.1	1.29	0.49	124.20	-	158.40	322.20
		III	0.1	0.29	0.10	29.92	-0.27	163.80	
3	AVERAGE	I + II	0.1	-4.62	0.94	-257.90	-	3.50	33.56
		III	0.1	0.58	0.51	30.64	0.05	30.06	
* 4	AVERAGE	I + II	0.1	-1.18	1.72	-37.89	-	23.61	134.20
		III	0.1	0.78	0.59	37.55	0.04	110.60	
*GRAND	AVERAGE	I + II	0.1	-0.52	7.09	-5.85	-	73.85	96.98
		III	0.1	1.02	0.80	37.64	-0.02	23.13	

*Based on single run only for S2, S4.

Table 9/ Best-Fit Driver Model Parameters, Parked Pole

Subject No.	Run No.	Phase	τ (s)	T_I (s)	T_L (s)	G_ψ	ΔS (m)	J $(deg)^2$	J_3 $(deg)^2$
3	5	I	0.3	2.38	0.83	92.96	-	3.88	31.45
		II	0.3	1.02	0	35.26	3.86	0.66	
		III	0.3	0.69	0.69	24.60	0.13	27.91	
3	6	I	0.5	0.21	0.37	30.78	-	5.27	91.39
		II	0.5	0.44	0	21.80	4.42	2.57	
		III	0.5	0.18	0.42	19.33	0.04	83.55	
3	7	I	0.5	0.17	0.40	29.75	-	57.05	112.0
		II	0.5	2.98	0	-64.04	-6.93	0.99	
		III	0.5	1.42	2.09	13.71	0.35	53.91	
3	8	I	0.1	-0.46	9.84	-2.92	-	1.42	19.10
		II	0.1	1.26	0	-64.80	-4.97	0.19	
		III	0.1	1.46	1.04	37.61	0.08	17.49	
1	AVERAGE	I	0.4	5.63	1.50	130.90	-	1.02	6.37
		II	0.4	1.93	0	5.45	13.80	0.69	
		III	0.4	1.64	1.77	13.25	0.43	4.66	
2	AVERAGE	I	0.2	-0.27	-105.7	0.23	-	6.48	15.26
		II	0.2	1.31	0	25.45	3.60	0.13	
		III	0.2	0.75	0.67	23.97	0.12	8.65	
3	AVERAGE	I	0.3	3.18	1.03	122.40	-	0.57	9.21
		II	0.3	2.57	0	-20.18	-20.4	0.11	
		III	0.3	0.55	0.66	23.11	0.06	8.53	
4	AVERAGE	I	0.2	-0.28	-12.90	1.72	-	8.21	51.61
		II	0.2	4.48	0	75.53	4.85	0.44	
		III	0.2	0.47	0.38	23.24	0.15	42.96	
GRAND	AVERAGE	I	0.3	-0.50	32.73	-0.83	-	2.00	8.29
		II	0.3	1.79	0	21.61	6.70	0.23	
		III	0.3	0.63	0.76	22.96	0.04	6.06	

Table 10/ Model Sensitivity Analysis, Subject 3, Long Preview, Averaged Run

Phase	τ (s)	TI (s)	TL (s)	Gψ	ΔS (m)	Sight Point (m)	J (deg)^2	$\frac{\Delta J\%}{\Delta\%}$
I	0.1	-0.63	2.58	-11.56	-	-	1.45	REF
	0.2	-1.43	1.53	-35.07			3.19	1.2
		-0.76					747	2575
			3.10				300	1034
				-13.87			88.5	305
II	0.1	1.89	-	44.16	4.10	40	2.09	REF
	0.2	1.46	-	30.34	5.53		0.94	0.6
		2.27					477	1142
				52.99			105	252
					4.92		329	786
		1.61		37.68	4.90	30	2.11	0.04
III	0.1	0.53	0.40	29.75	0.04	20	10.99	REF
	0.2	0.62	0.56	27.29	0.05		11.68	0.1
		0.64					70.30	32
			0.48				85.70	39
				35.70			85.70	39
					0.05		11.20	0.1
		0.07	-0.26	21.01	0.18	30	12.80	0.7

Figure 1/ Test Vehicle on Track

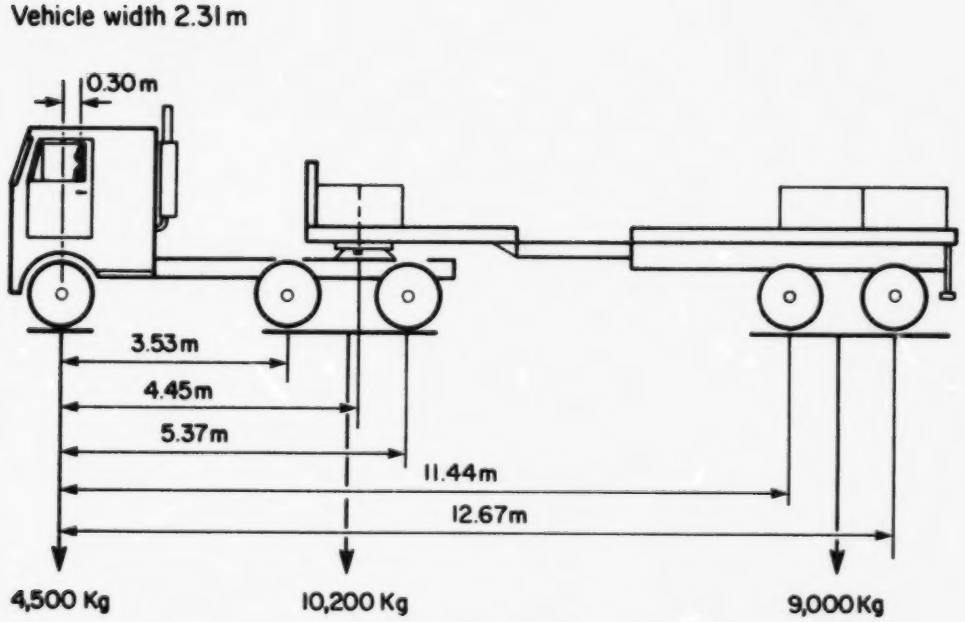

Figure 2/ Test Vehicle Configuration

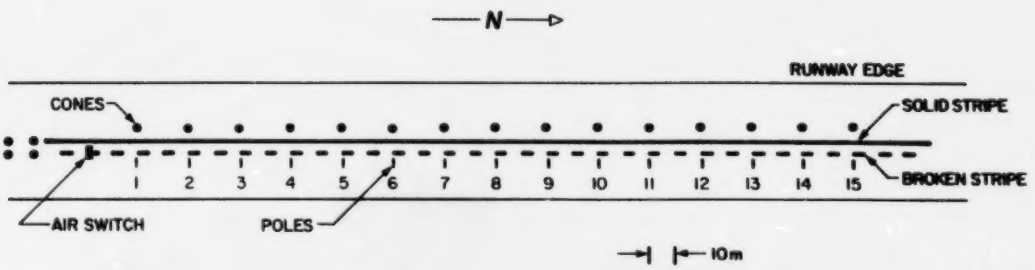

Figure 3/ Test Area Layout

Figure 4/ Active Pole Begins to Fall (Designated Pole Case)

Figure 5/ Obstacle Avoidance Manoeuvre
Begins (Designated Pole Case)

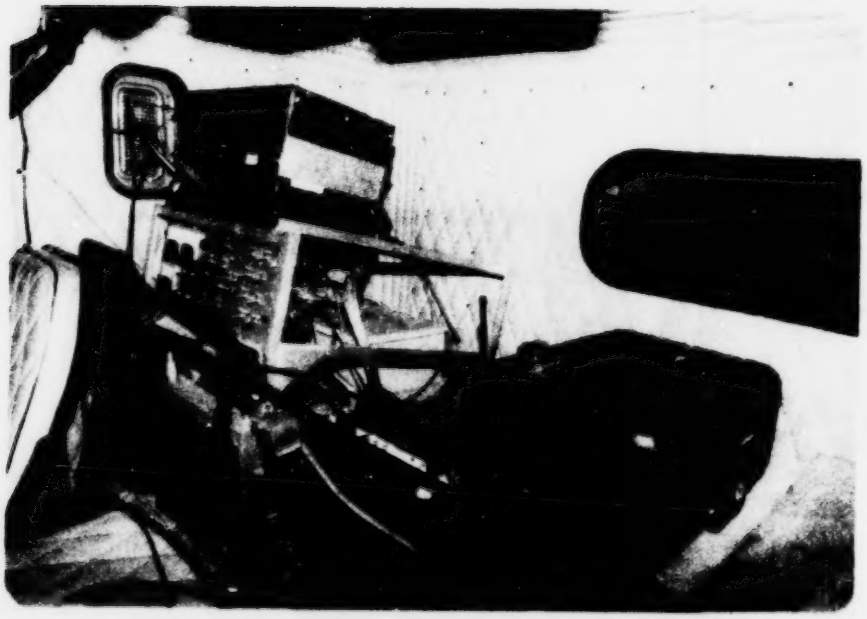

Figure 6/ Humphrey Instrumentation Package
and Data Acquisition Equipment

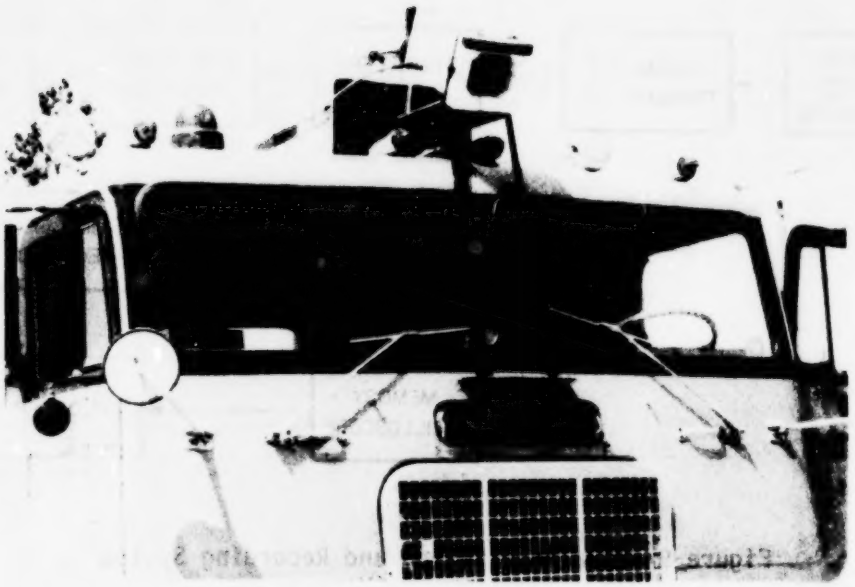

Figure 7/ Lane Tracker Installation

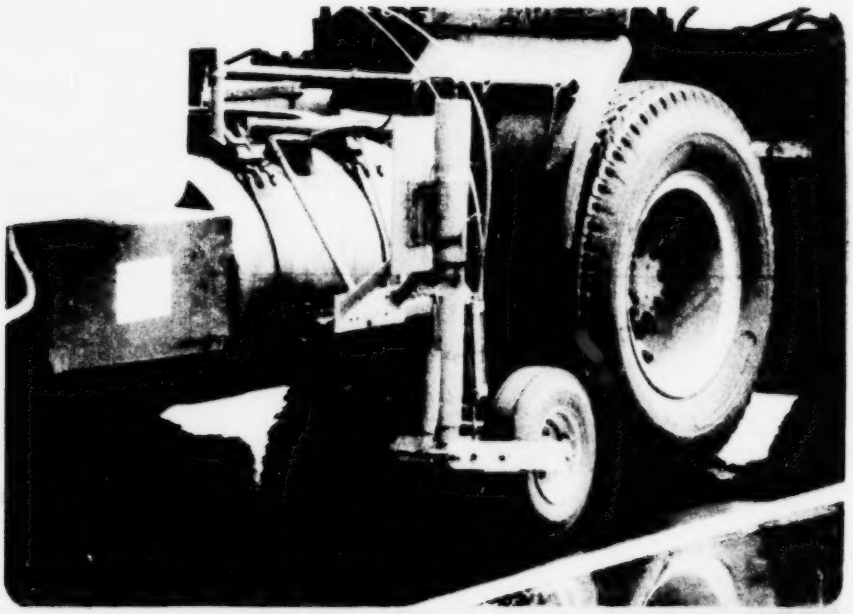

Figure 8/ Sidewall Distance/Speed/Sideslip Sensor

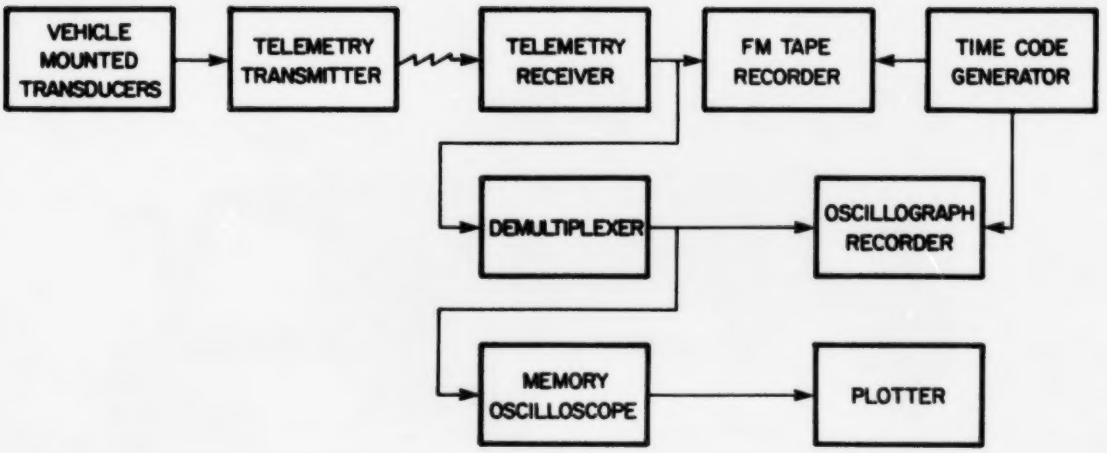

Figure 9/ Data Acquisition and Recording System

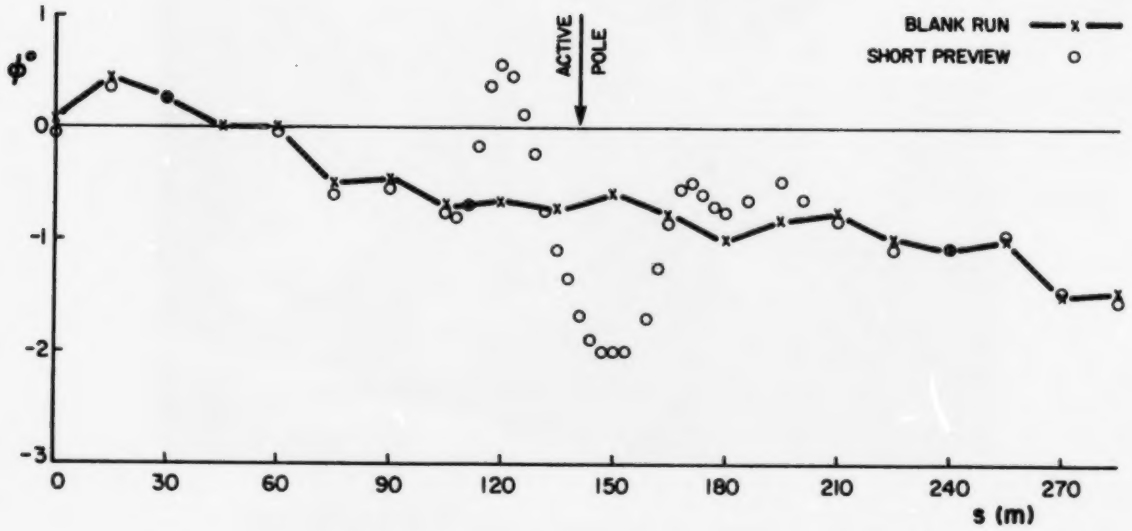

Figure 10/ Sensed Vehicle Roll Angle (Driver 1)

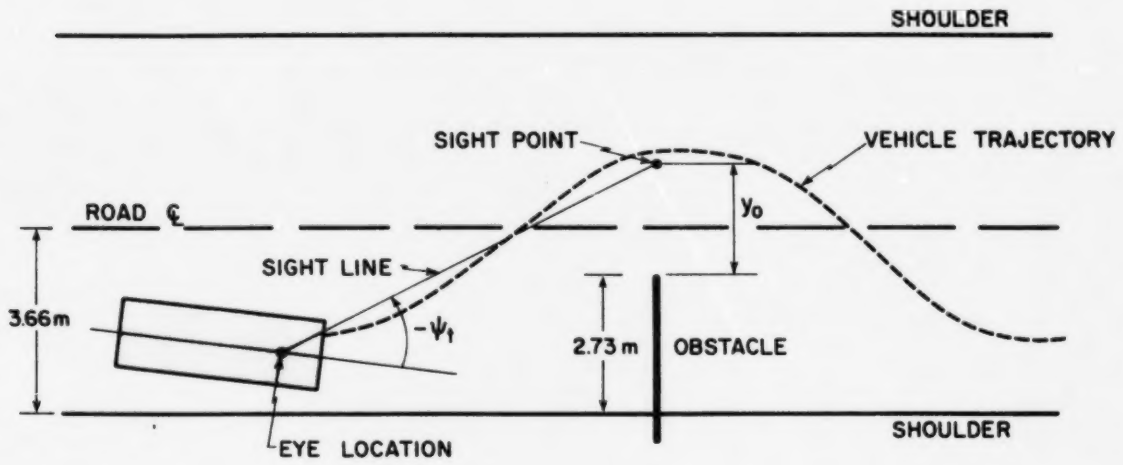

Figure 11/ Obstacle Avoidance Manoeuvre

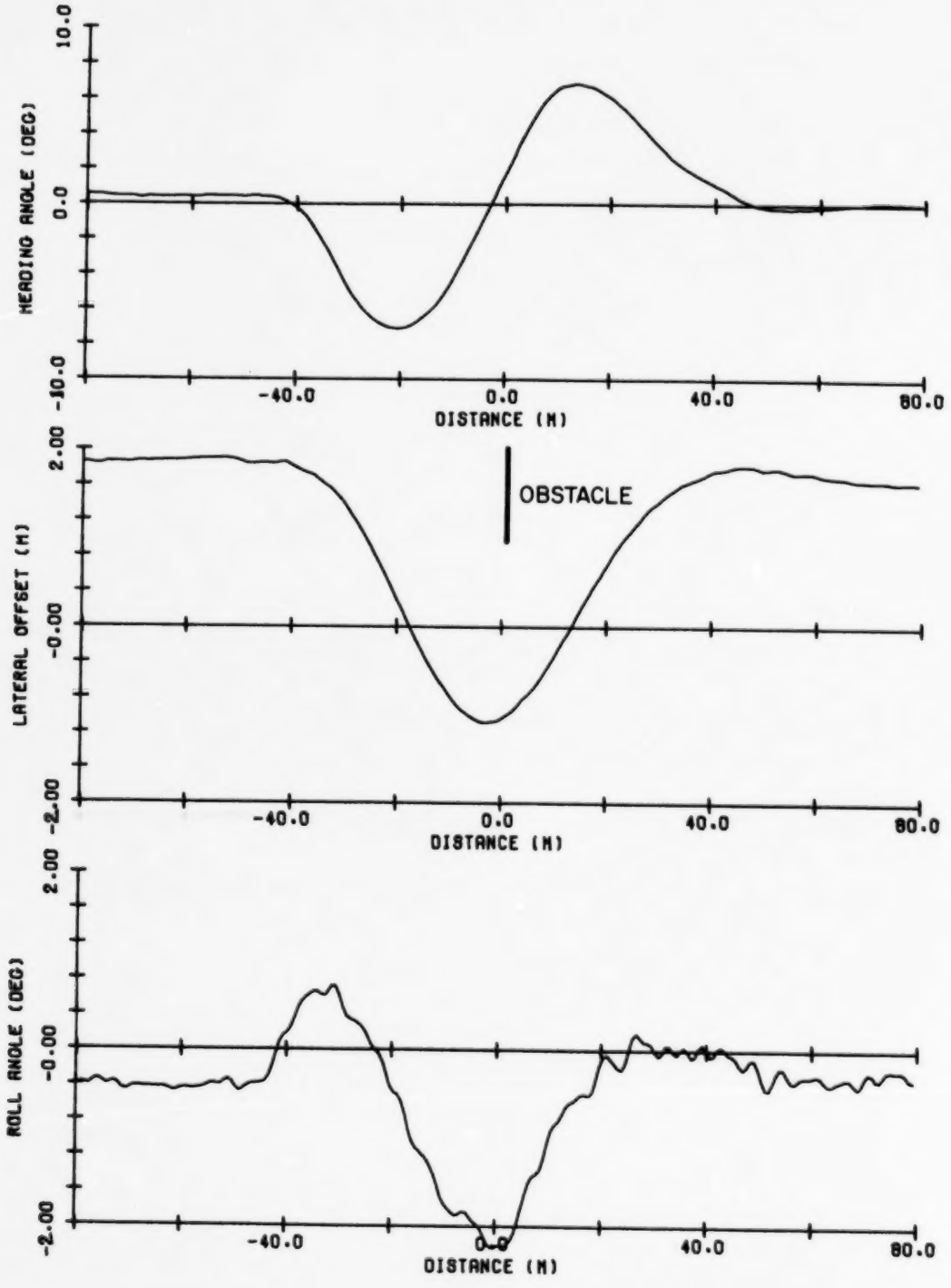

Figure 12/ Typical Recorded Experimental Data
Subject 3, Long Preview, Run No. 5

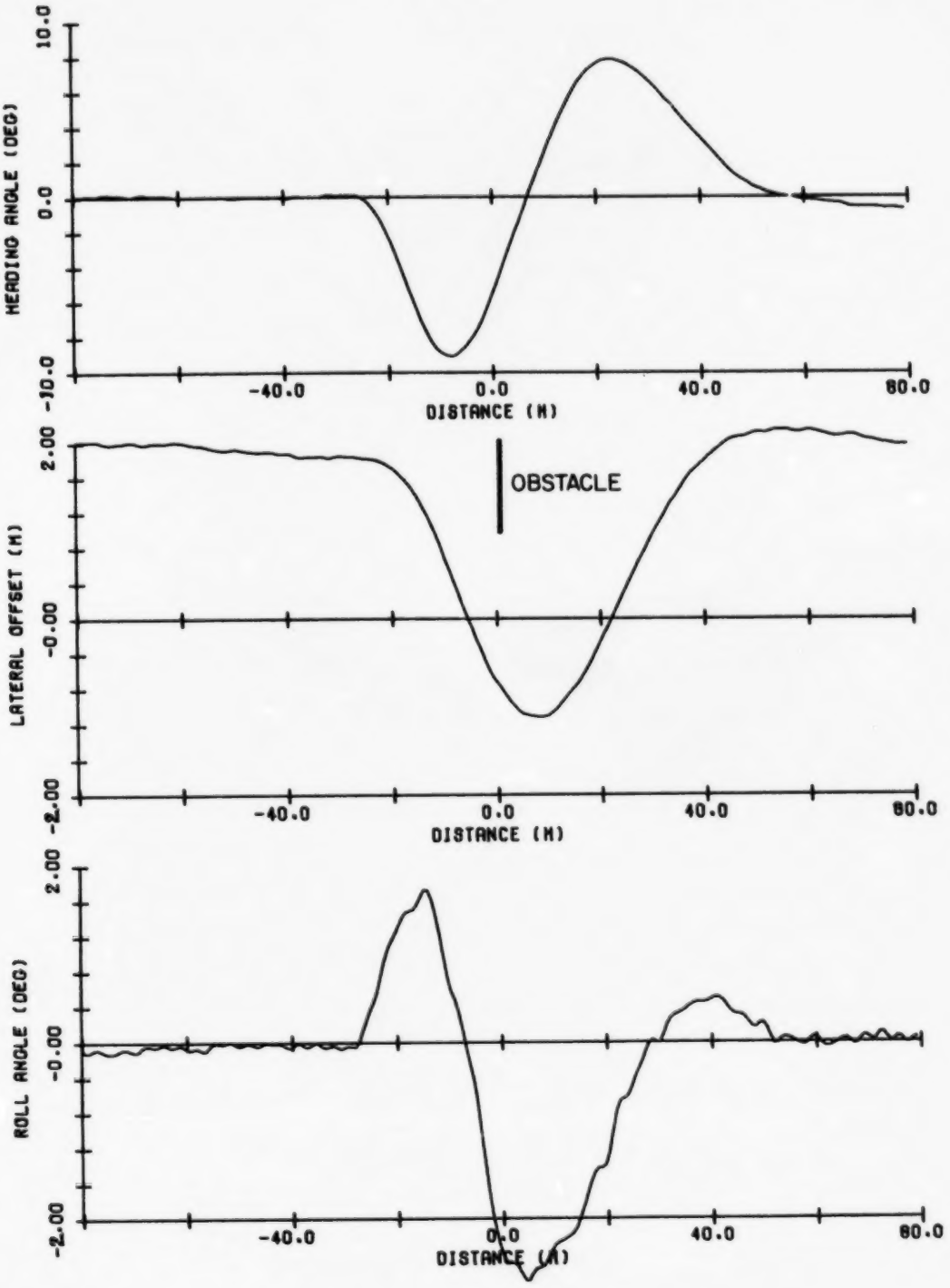

Figure 13/ Typical Recorded Experimental Data,
Subject 3, Short Preview, Run No. 5

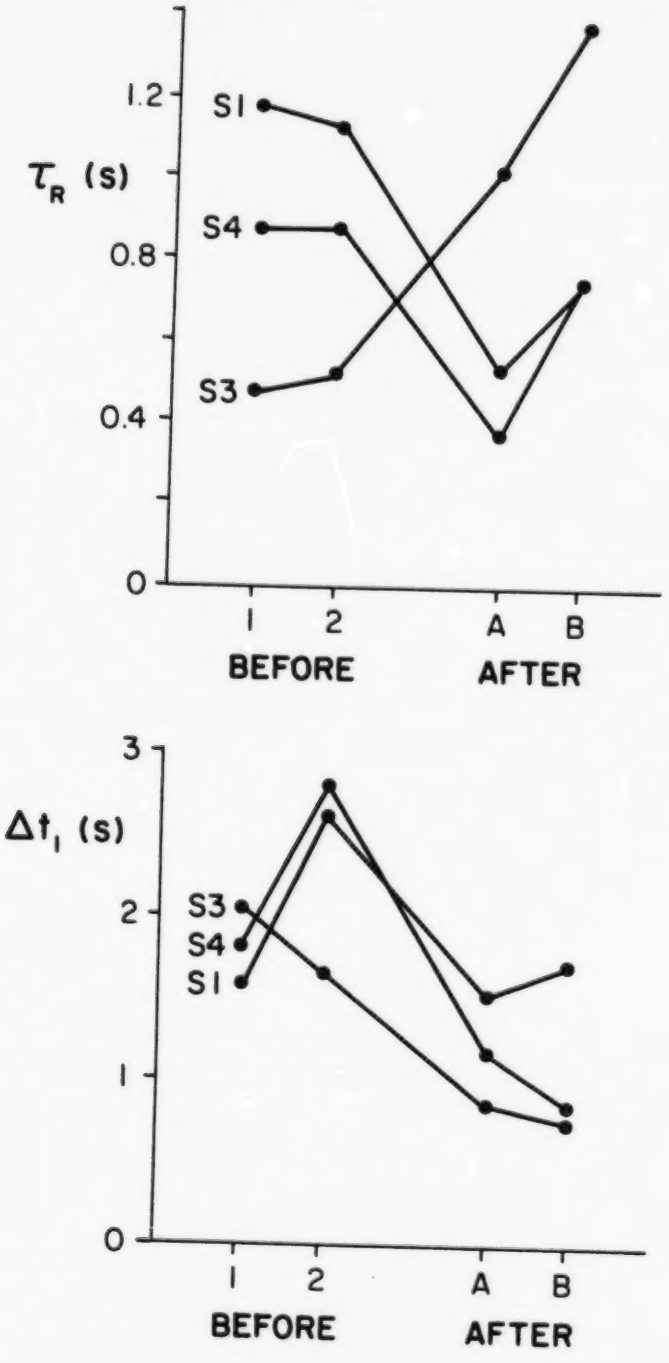

Figure 14/ Training Effects, Long Preview

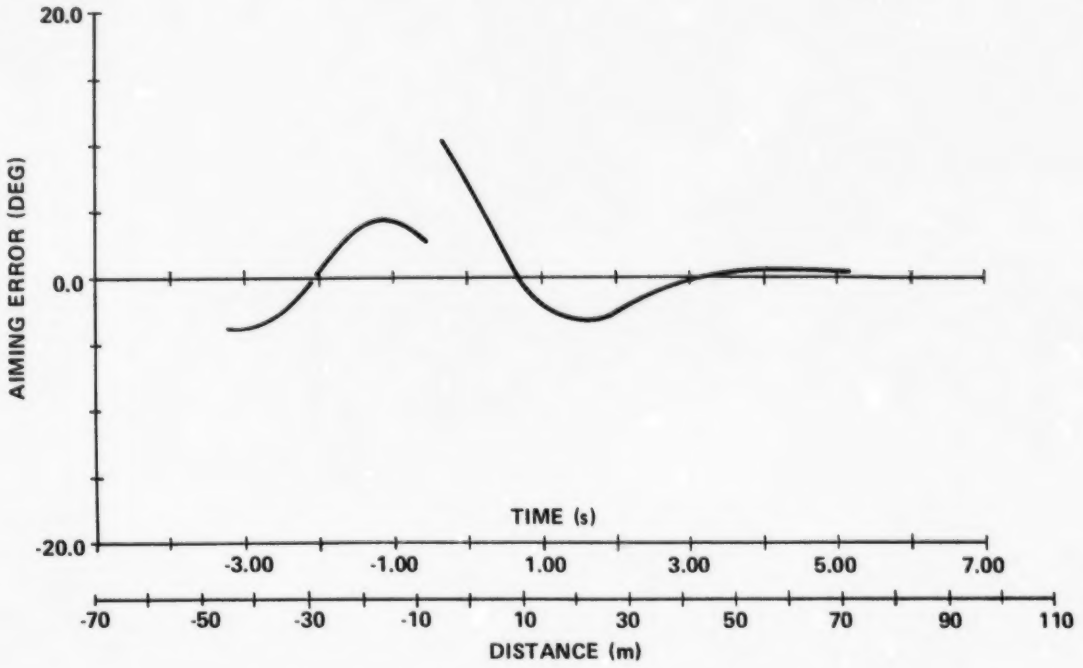

Figure 15/ Typical ψ_t Aiming Error Record, Subject 3, Long Preview, Averaged Run

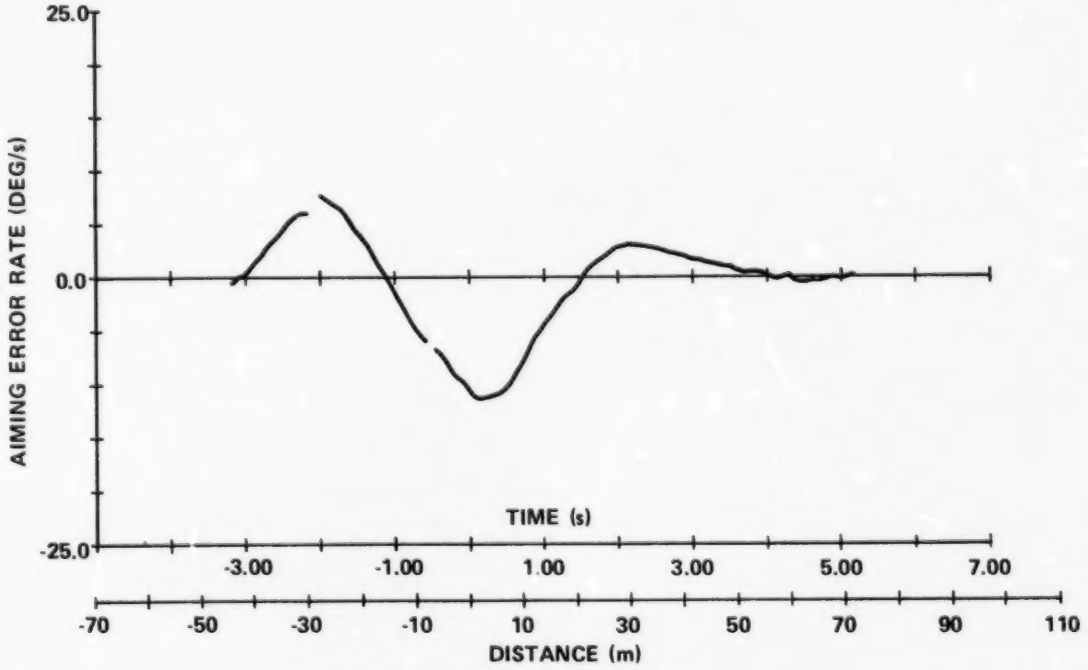

Figure 16/ Typical ψ_t Aiming Error Rate Record, Subject 3, Long Preview, Averaged Run

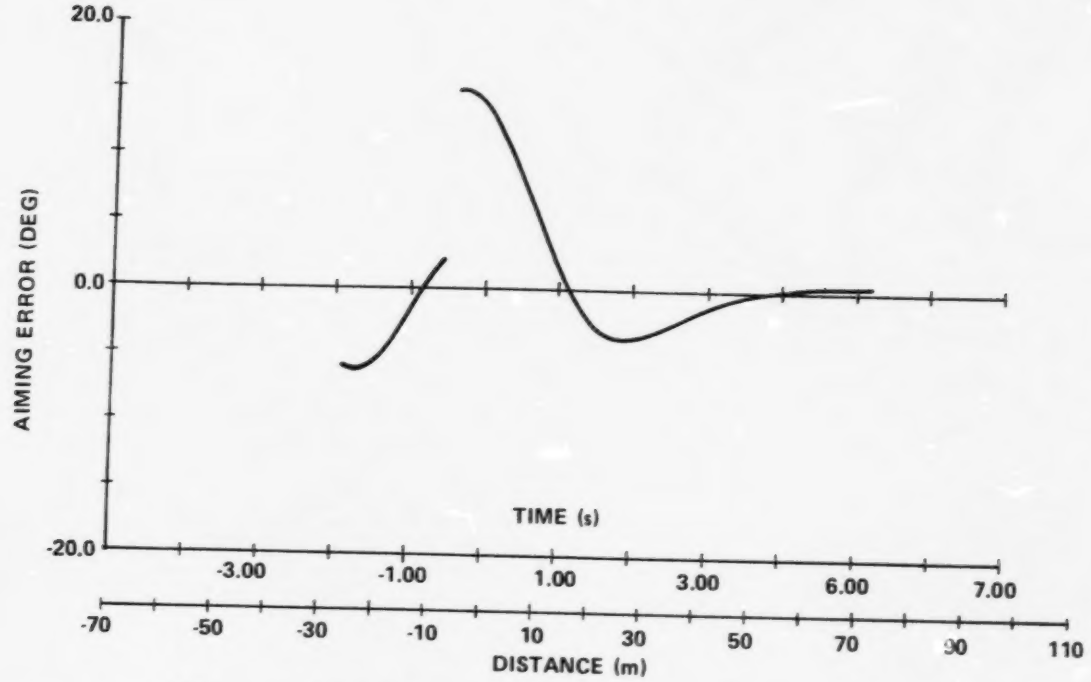

Figure 17/ Typical ψ_t Aiming Error Record,
Subject 3, Short Preview, Averaged Run

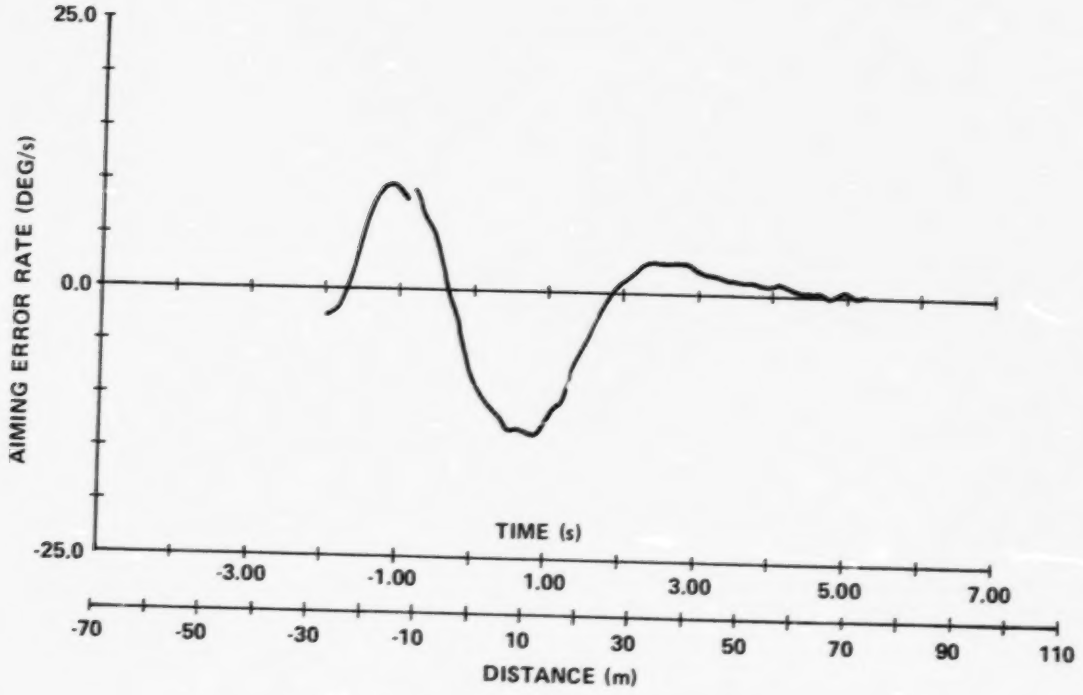

Figure 18/ Typical ψ_t Aiming Error Rate Record,
Subject 3, Short Preview, Averaged Run

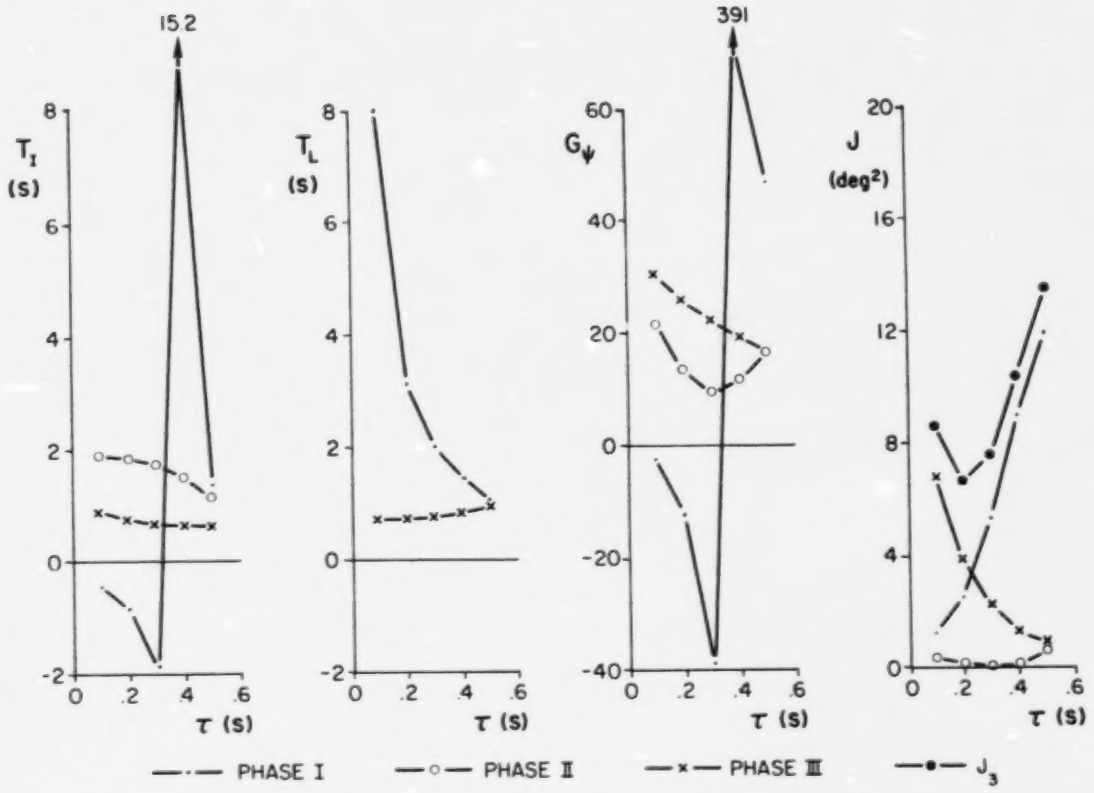

Figure 19/ The Effect of τ Variation on Driver Model Parameters, Long Preview, Grand Averaged Run

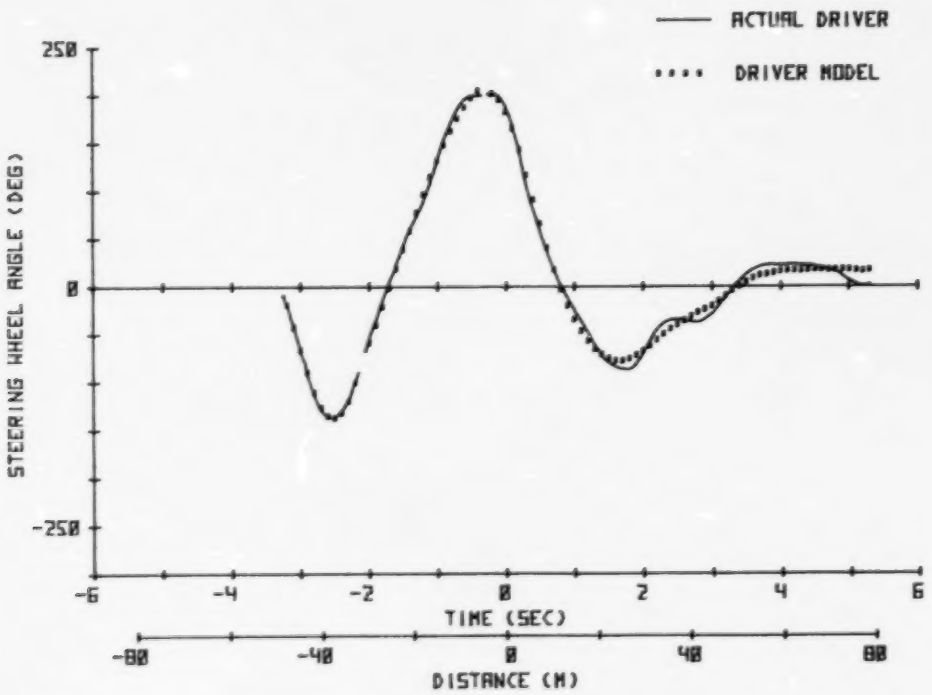

Figure 20/ Steering Wheel Response, Subject 3, Long Preview, Run No. 5

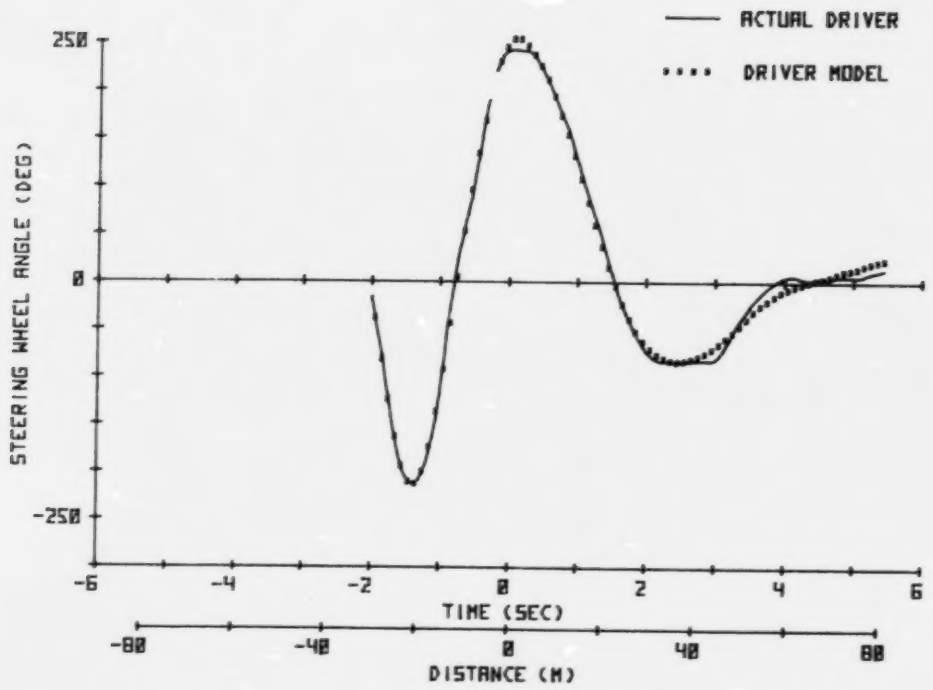

Figure 21/ Steering Wheel Response, Subject 3,
Short Preview, Run No. 5

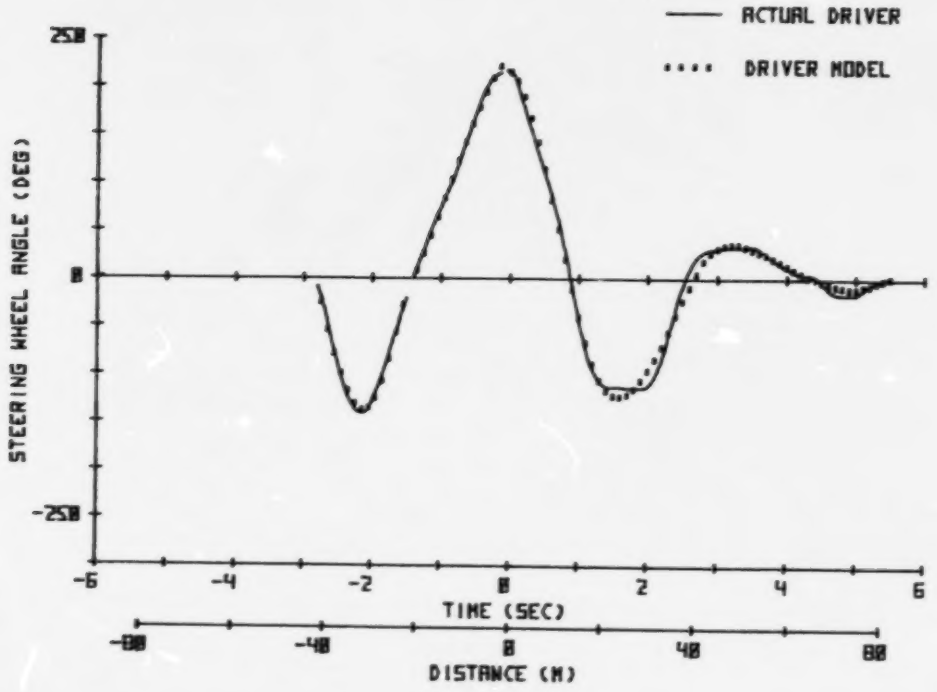

Figure 22/ Steering Wheel Response, Subject 3,
Designated Pole, Long Preview, Run No. 5

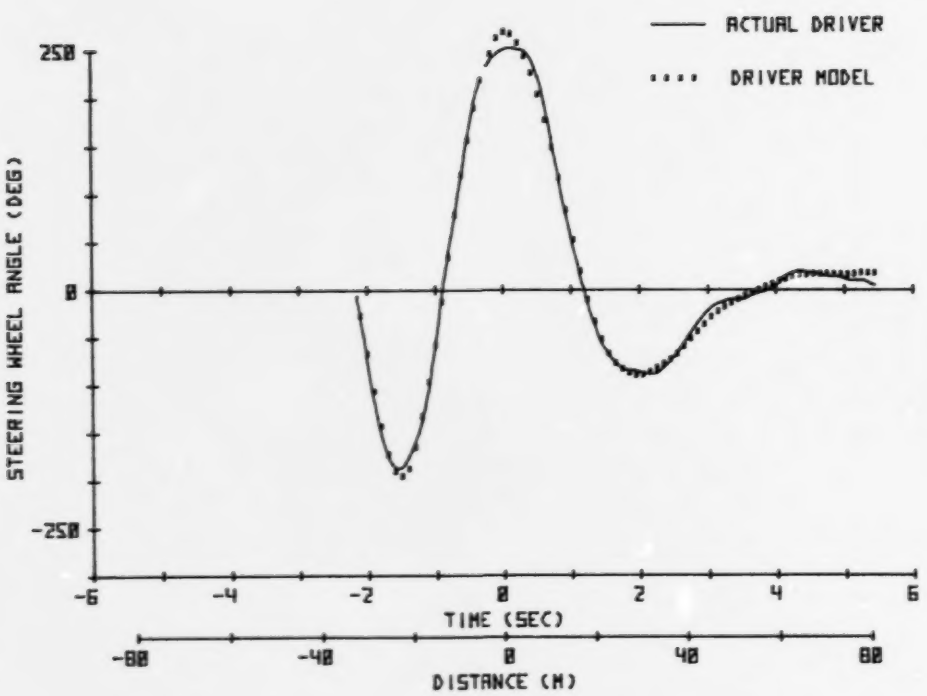

Figure 23/ Steering Wheel Response, Subject 3, Designated Pole, Short Preview, Run No. 5

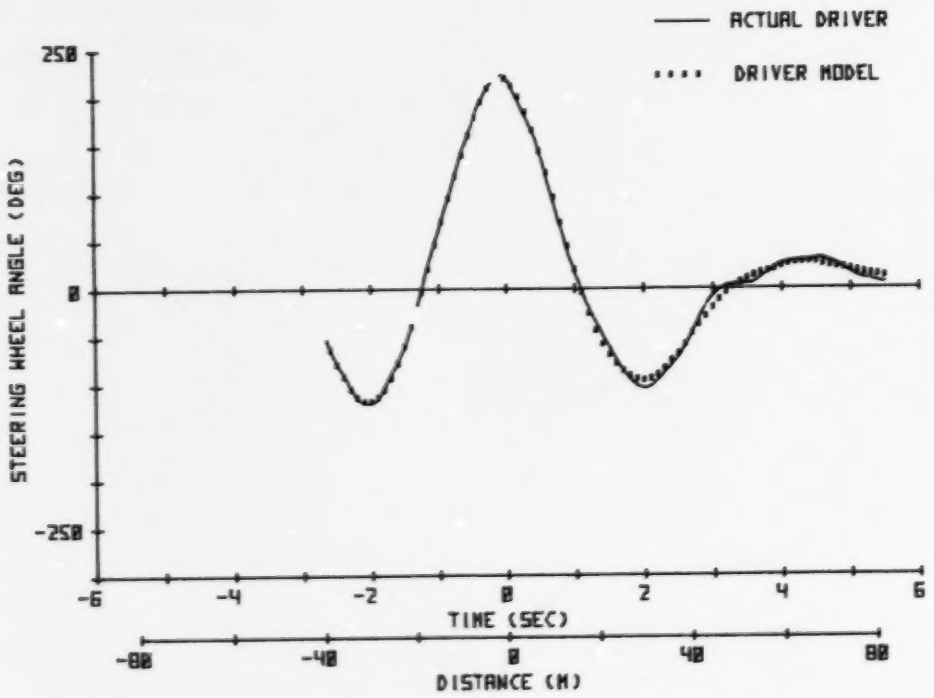

Figure 24/ Steering Wheel Response, Subject 3, Parked Pole, Run No. 5

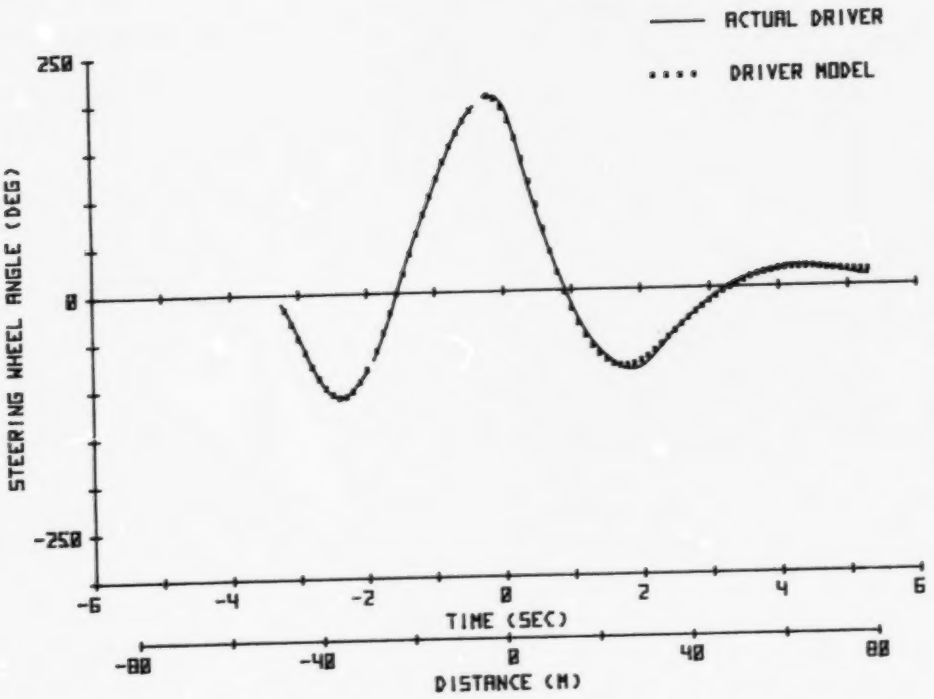

Figure 25/ Steering Wheel Response, Subject 3, Long Preview, Averaged Run

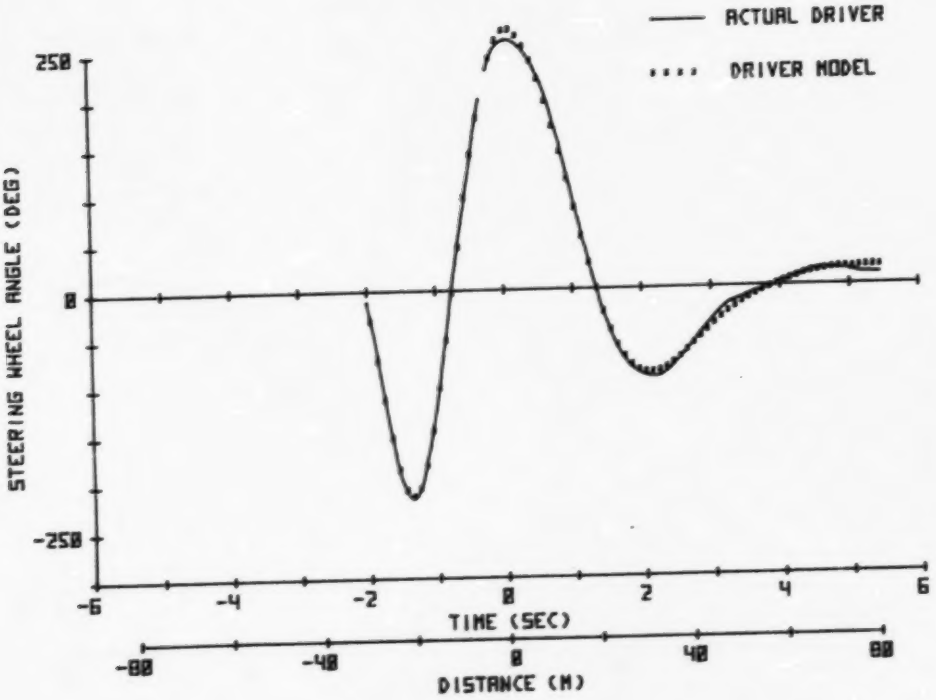

Figure 26/ Steering Wheel Response, Subject 3, Short Preview, Averaged Run

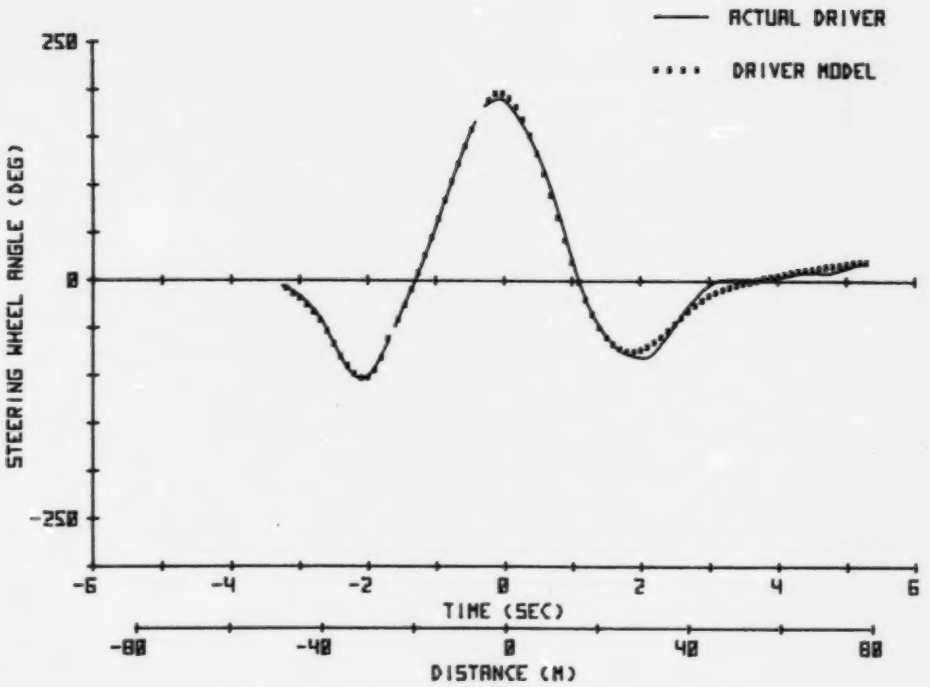

Figure 27/ Steering Wheel Response, Subject 3, Designated Pole, Long Preview, Averaged Run

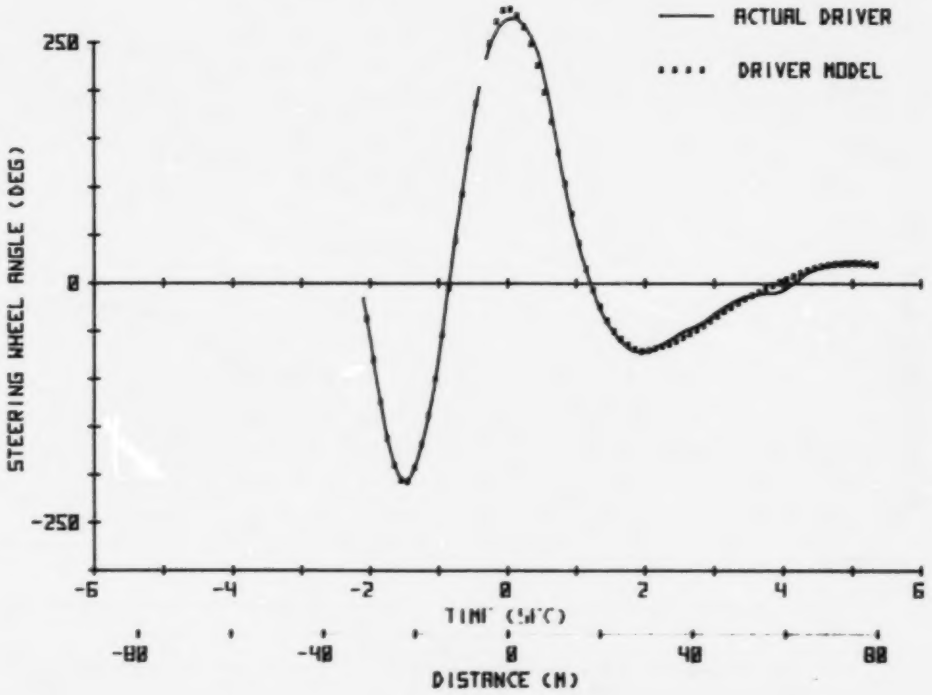

Figure 28/ Steering Wheel Response, Subject 3, Designated Pole, Short Preview, Averaged Run

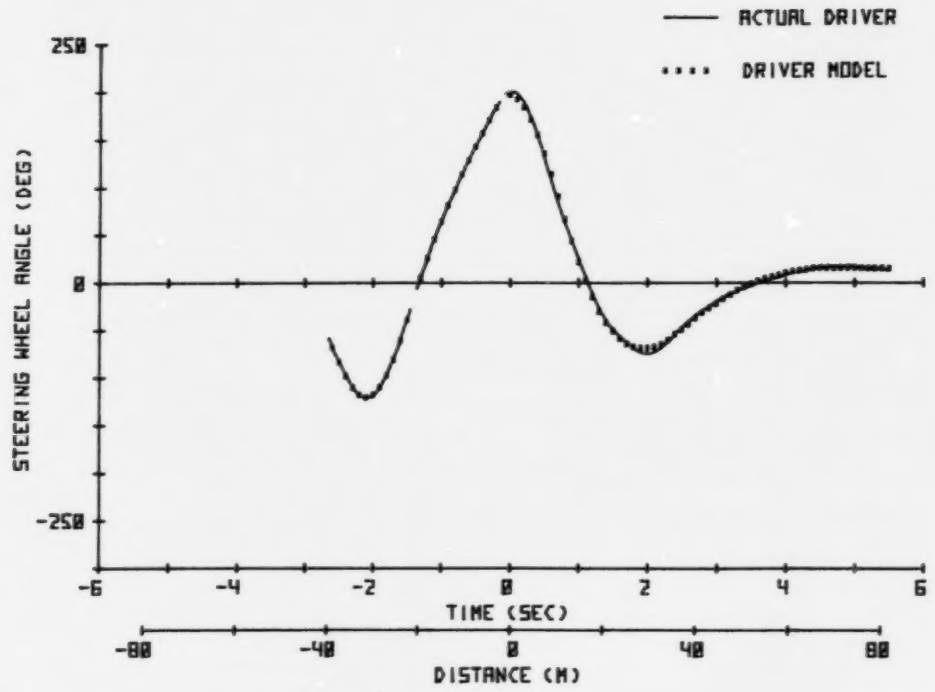

Figure 29/ Steering Wheel Response, Subject 3,
Parked Pole, Averaged Run

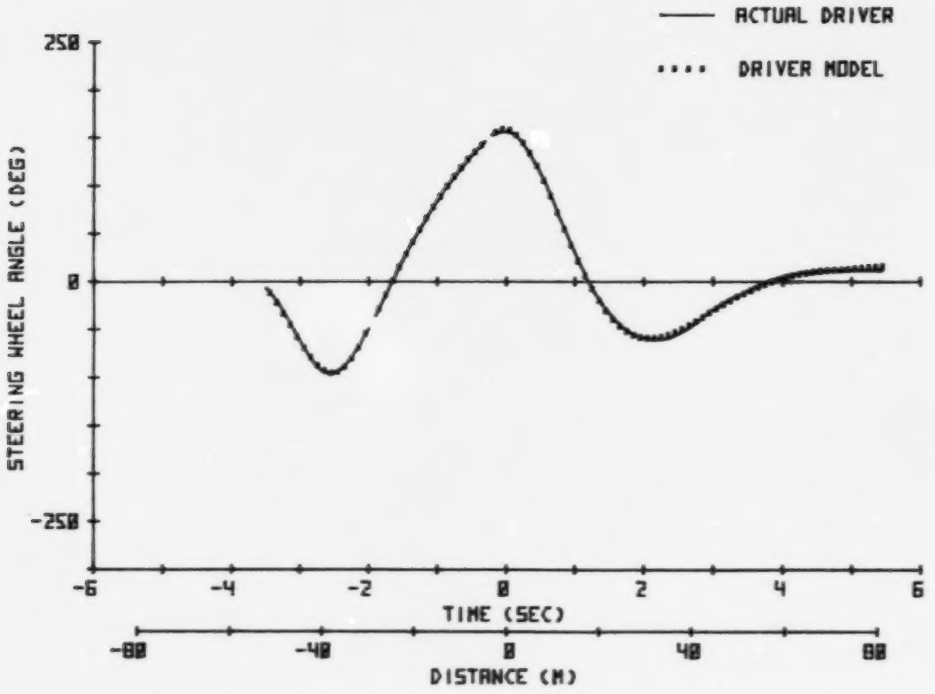

Figure 30/ Steering Wheel Response,
Long Preview, Grand Average Run

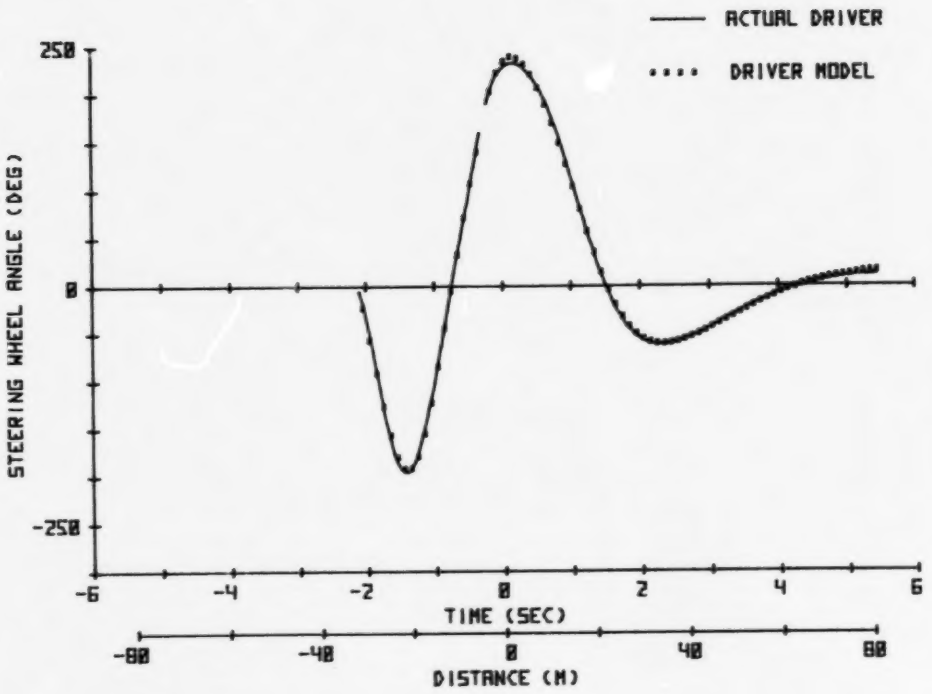

Figure 31/ Steering Wheel Response,
Short Preview, Grand Average Run

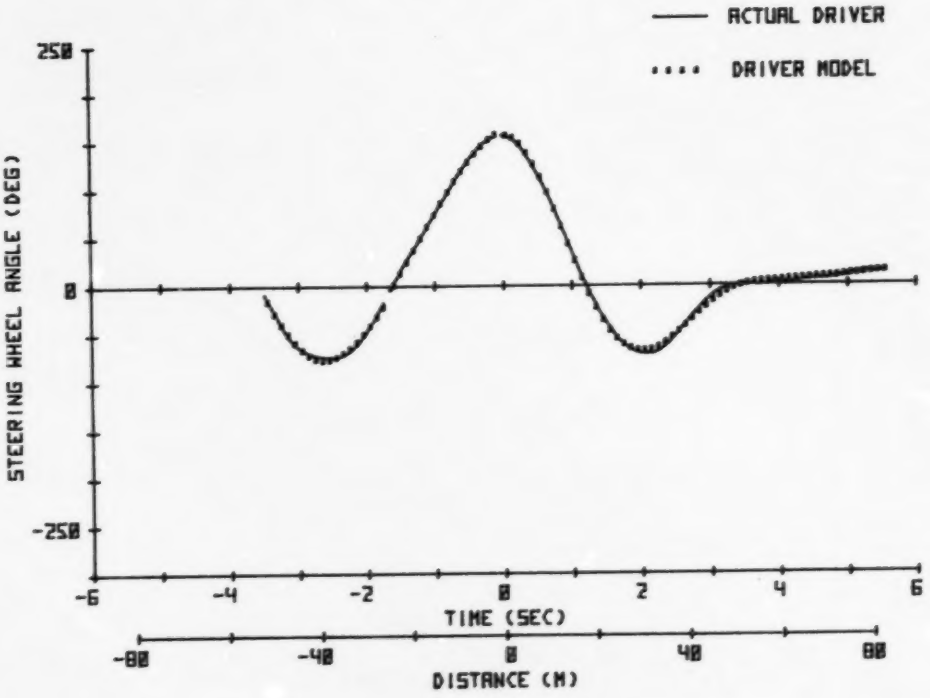

Figure 32/ Steering Wheel Response, Designated Pole,
Long Preview, Grand Average Run

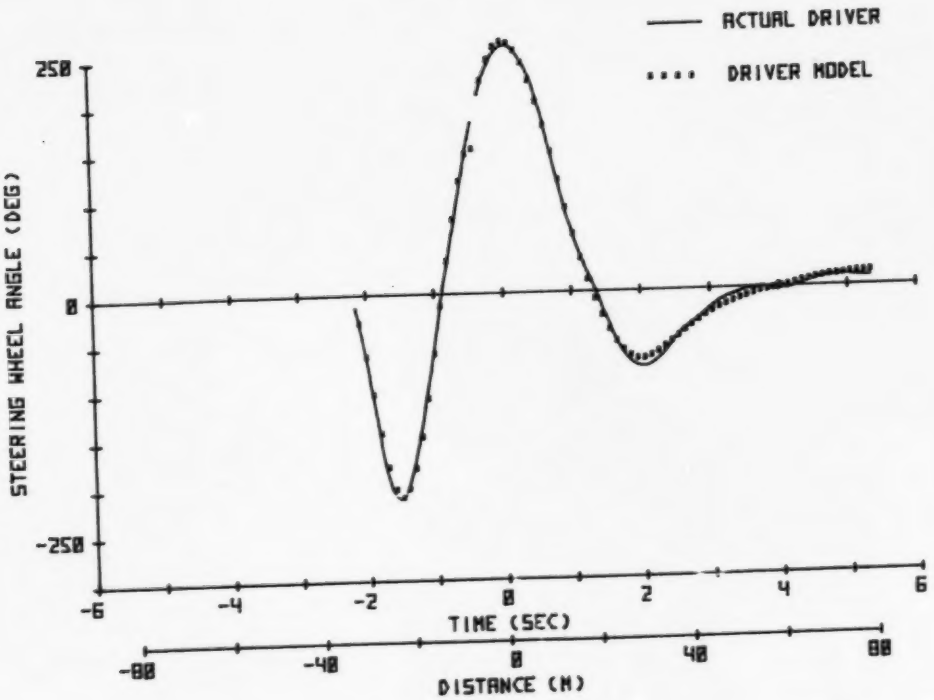

Figure 33/ Steering Wheel Response, Designated Pole, Short Preview, Grand Average Run

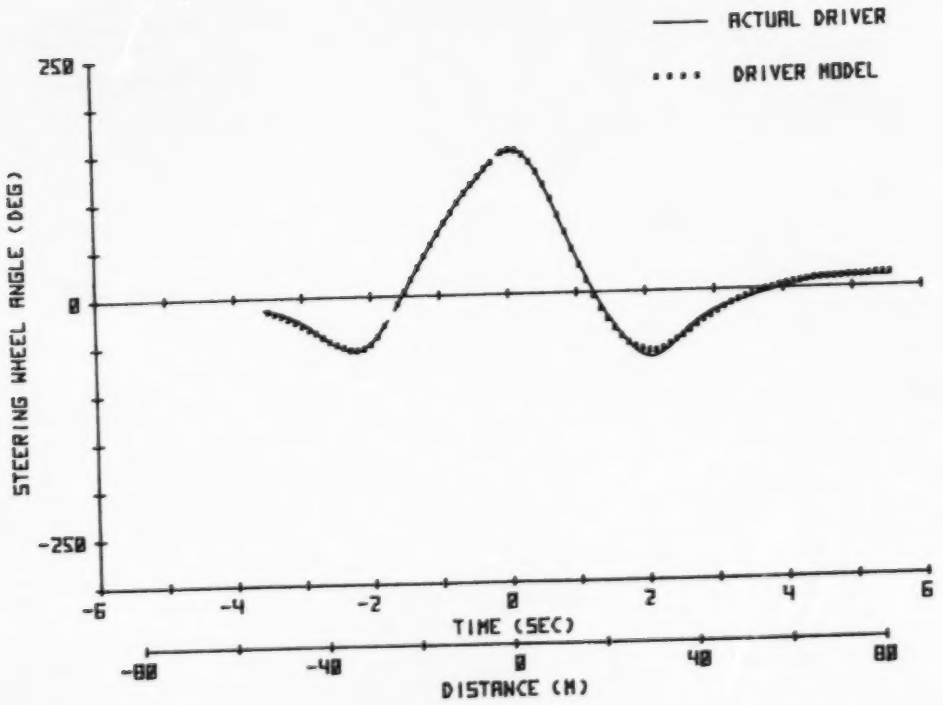

Figure 34/ Steering Wheel Response, Parked Pole, Grand Average Run

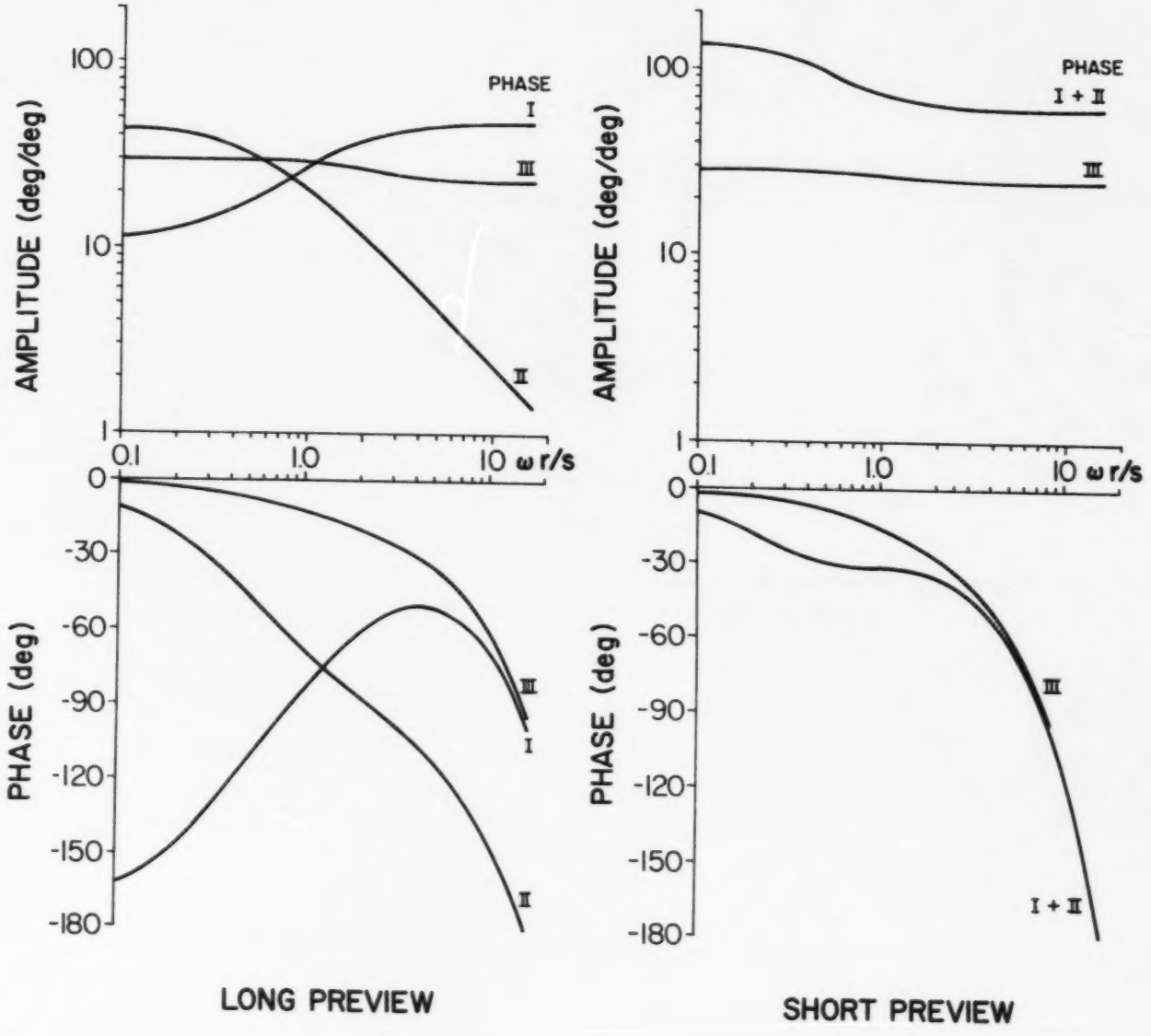

Figure 35/ Frequency Response Curves for the Driver Model, Subject 3, Long and Short Preview, Averaged Run

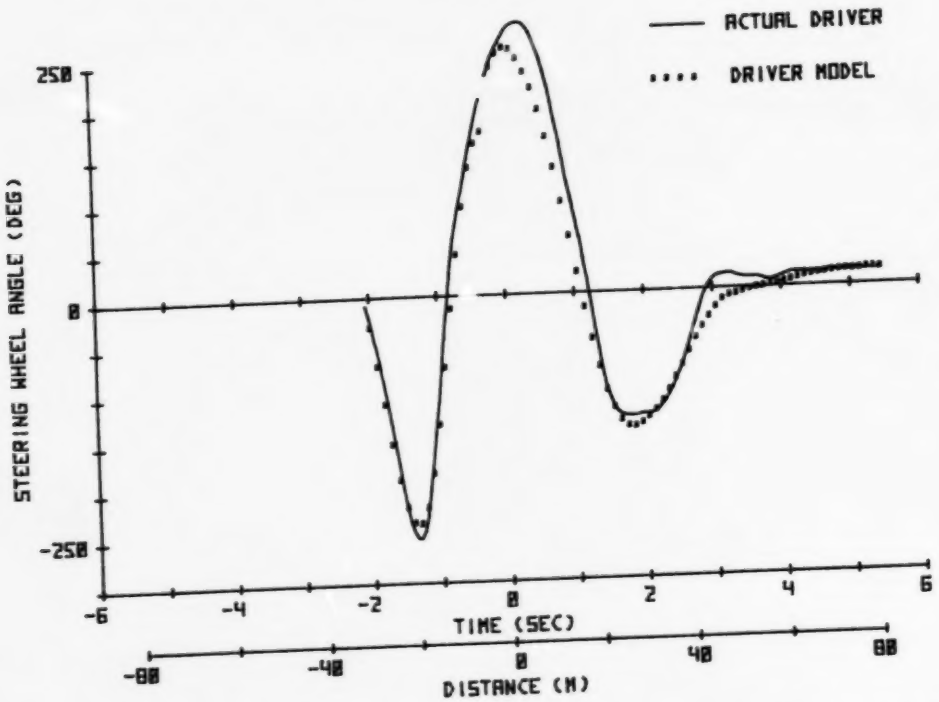

Figure 36/ Steering Wheel Response, Subject 3, Short Preview, Run No. 8 Fitted by Subject 3 Averaged Run Model

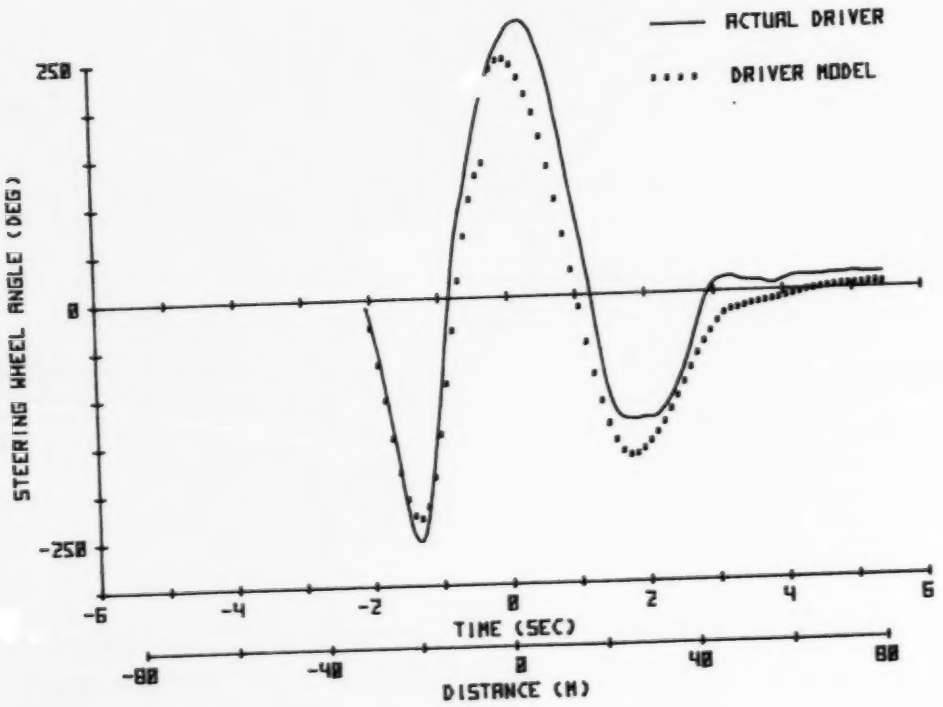

Figure 37/ Steering Wheel Response, Subject 3, Short Preview, Run No. 8 Fitted by Grand Averaged Run Model

APPENDIX A/ Lane Tracker Measurements

Consider the situation depicted in Figure A.1. Here F_I represents an Earth-fixed reference frame with its x-axis along the road centre stripe and its z-axis pointing vertically downward. Let F_B be an axis system fixed to the tractor with its x-axis along the roll axis of the vehicle (assumed to lie in the tractor's vertical plane of symmetry) and its z-axis passing through the tractor's centre of gravity (which also lies in the vertical plane of symmetry). Let F_C be the lane tracker axis system with its x-axis along the camera's optical axis and its xy plane parallel to the bottom of the camera.

The lane tracker output can be used to generate the angle β between the camera's optical axis and the line in the xy plane of F_C which joins the origin of F_C, O, to the point S where this xy plane intersects the road centre stripe.

$$\beta = \angle POS \tag{A.1}$$

and P is the point where the optical axis of the camera intersects the road surface (the xy plane of F_I).

Let the origin of F_B in F_I coordinates be:

$$\begin{bmatrix} x_b \\ y_b \\ z_b \end{bmatrix} \tag{A.2}$$

Since the x-axis of F_B is assumed to be the roll axis, then z_b is a known constant. Let the origin of F_C in F_I coordinates be:

$$\begin{bmatrix} x_c \\ y_c \\ z_c \end{bmatrix} \tag{A.3}$$

and the origin of F_c in F_B coordinates be

$$\begin{bmatrix} x_d \\ y_d \\ z_d \end{bmatrix} = \begin{bmatrix} x_d \\ 0 \\ z_d \end{bmatrix} \tag{A.4}$$

(In the present case we have positioned the lane tracker so that $y_d = 0$.)

Let the transformation matrices be:

$$\underline{L}_{IB},\ \underline{L}_{BC} \text{ and } \underline{L}_{IC} \tag{A.5}$$

where $\underline{L}_{IC} = \underline{L}_{IB}\underline{L}_{BC}$

Thus, it can be shown that:

$$\begin{bmatrix} x_c \\ y_c \\ z_c \end{bmatrix} = \begin{bmatrix} x_b \\ y_b \\ z_b \end{bmatrix} + \underline{L}_{IB}\begin{bmatrix} x_d \\ 0 \\ z_d \end{bmatrix} \tag{A.6}$$

Let ϕ, θ, ψ be the Euler angles which carry F_I into F_B and ϕ_i, θ_i, ψ_i be the Euler angles which carry F_B into F_c [3]. We will deal with the case where:

$$\theta = \phi_i = \psi_i \equiv 0 \tag{A.7}$$

and

$$|\phi| << 1 \tag{A.8}$$

It then follows that:

$$\underline{L}_{IB} = \begin{bmatrix} \cos\psi & -\sin\psi & \phi\sin\psi \\ \sin\psi & \cos\psi & -\phi\cos\psi \\ 0 & \phi & 1 \end{bmatrix} \tag{A.9}$$

and

$$\underline{L}_{BC} = \begin{bmatrix} \cos\theta_i & 0 & \sin\theta_i \\ 0 & 1 & 0 \\ -\sin\theta_i & 0 & \cos\theta_i \end{bmatrix} \tag{A.10}$$

Let the location of the tractor's centre of gravity in F_B coordinates be:

$$\begin{bmatrix} 0 \\ 0 \\ z_{cg} \end{bmatrix} \tag{A.12}$$

Thus, the location of the tractor's centre of gravity in F_I coordinates is:

$$\begin{bmatrix} \Delta x \\ \Delta y \\ \Delta z \end{bmatrix} = \begin{bmatrix} x_b \\ y_b \\ x_b \end{bmatrix} + \underline{L}_{IB} \begin{bmatrix} 0 \\ 0 \\ z_{cg} \end{bmatrix}$$

$$= \begin{bmatrix} x_b \\ y_b \\ z_b \end{bmatrix} + \begin{bmatrix} z_{cg}\phi\sin\psi \\ -z_{cg}\phi\cos\psi \\ z_{cg} \end{bmatrix} \tag{A.13}$$

Thus, the desired measurement giving the lateral distance of the tractor's centre of gravity from the road stripe is:

$$y = y_b - z_{cg}\phi\cos\psi \tag{A.14}$$

Only the value of y_b on the right-hand side of Equation A.14 is unknown. From Equation A.6 it is found that:

$$y_b = y_c - x_d\sin\psi + z_d\phi\cos\psi \tag{A.15}$$

In Equation A.15, only y_c is unknown. An expression for y_c in terms of the lane tracker output β can be found by deriving an equation for the line OS in F_I. This line passes through the point O and is parallel to the unit vector $\underline{e}$ (see Figure A.1) with components in F_c given by:

$$\begin{bmatrix} \cos\beta \\ \sin\beta \\ 0 \end{bmatrix} \tag{A.16}$$

The components of $\underline{e}$ in F_I are:

$$\underline{e}_I = \begin{bmatrix} e_{11} \\ e_{12} \\ e_{13} \end{bmatrix}$$

$$= \underline{L}_{IC} \begin{bmatrix} \cos\beta \\ \sin\beta \\ 0 \end{bmatrix}$$

$$= \underline{L}_{IB}\,\underline{L}_{BC} \begin{bmatrix} \cos\beta \\ \sin\beta \\ 0 \end{bmatrix}$$

$$= \begin{bmatrix} \cos\psi\cos\theta_i\cos\beta - \phi\sin\psi\sin\theta_i\cos\beta - \sin\psi\sin\beta \\ \sin\psi\cos\theta_i\cos\beta + \phi\cos\psi\sin\theta_i\cos\beta + \cos\psi\sin\beta \\ \phi\sin\beta - \sin\theta_i\cos\beta \end{bmatrix} \qquad \text{(A.17)}$$

Thus, the equation for the coordinates of a general point on the line OS expressed in F_I coordinates (x^1, y^1, z^1) is:

$$\begin{bmatrix} x^1 \\ y^1 \\ z^1 \end{bmatrix} = \begin{bmatrix} x_C \\ y_C \\ z_C \end{bmatrix} + t\,\underline{e}_I \qquad \text{(A.18)}$$

where t is a free parameter.

Now, one other point on this line is S, with coordinates in F_I given by:

$$\begin{bmatrix} x_S \\ 0 \\ 0 \end{bmatrix} \qquad \text{(A.19)}$$

Substituting Equation A.19 into Equation A.18 gives:

$$\begin{bmatrix} x_s \\ 0 \\ 0 \end{bmatrix} = \begin{bmatrix} x_c \\ y_c \\ z_c \end{bmatrix} + t\underline{e}_I \tag{A.20}$$

From the y and z coordinate terms in Equation A.20 it follows that:

$$\begin{aligned} y_c &= - te_{I2} \\ z_c &= - te_{I3} \end{aligned} \tag{A.21}$$

or $$y_c = z_c e_{I2}/e_{13} \tag{A.22}$$

From Equation A.6 it is found that:

$$z_c = z_b + z_d \tag{A.23}$$

Combining Equations A.22 and A.23:

$$y_c = (z_b + z_d)\, e_{I2}/e_{I2} \tag{A.24}$$

Thus, from Equations A.14, A.15, A.17, and A.24 it follows that:

$$\begin{aligned} y = &\left(z_b + z_d\right)\left(\frac{\sin\psi\cos\theta_i\cos\beta + \phi\cos\psi\sin\theta_i\cos\beta + \cos\psi\sin\beta}{\phi\sin\beta - \sin\theta_i\cos\beta}\right) \\ &-x_d\sin\psi + (z_d - z_{cg})\,\phi\cos\psi \end{aligned} \tag{A.25}$$

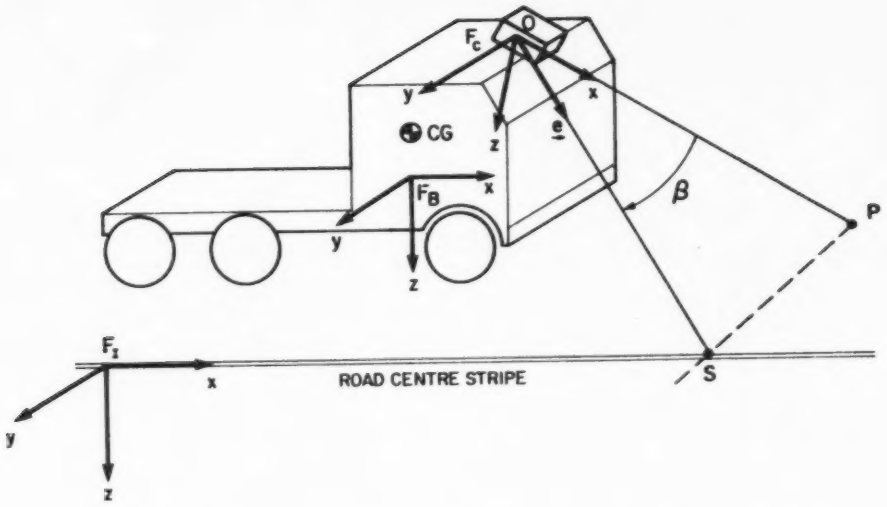

Figure A.1/ Lane Tracker Geometry

Figure A.1/ Lane Tracker Geometry

APPENDIX B/ Active Pole Triggering Mechanism

The active pole can be made to fall at a controlled distance in front of the truck by using an on-board pole base detecting system. During the present tests, this distance was either 32.5 m or 52.5 m in front of the tractor's bumper when it was travelling at the designated speed of 50 km/h (13.9 m/s). To achieve a preview distance of 32.5 m when, for example, Pole 8 is the active pole, the on-board experimenter presses the trigger button after passing Pole 5 and before reaching Pole 6. He has about 1.4 s in which to do this and it is done in such a manner that it goes undetected by the driver. This starts the ultrasonic speaker (transmitter/receiver) of a Polaroid Ultrasonic Ranging System located on the front bumper as shown in Figure B.1, which continues to operate for 2.0 s. This module detects the presence and range of distant objects by transmitting 40 kHz acoustic pulses (40 times/second) and then listening for the reflected signal. By mounting the system to look sideways, it detects the presence of the pole mounting bases. In the present example, the system detects the presence of Pole 6 (the triggering pole). False signals from objects beyond the line of poles are prevented by setting the receiver to ignore returns from objects further away than 2 m. Upon detecting Pole 6, the system activates a radio transmitter that sends a signal to a receiver located in the base unit of active Pole 8. A time delay circuit delays this triggering signal sufficiently so that the active pole is released to fall when the front bumper of the truck is 32.5 m from Pole 8 (assuming that the truck has a speed of 13.9 m/s).

Tests have indicated that the system employing the Polaroid module produces reliable indications of the presence of a pole base. When this indication is received, it is found that the pole base is located within a ± 20 cm band ahead of or behind the tractor's front bumper.

Generally this system worked very well. When it was found that the right front tractor wheel could splash water forward into the field of the ultrasonic sensor and cause early triggering, a splash guard was installed (see Figure B.1). A fault in the system at one stage during

the testing of Driver 2 necessitated the direct detection of the triggering pole by the on-board experimenter. Measurements indicate that in this case the pole-detected signal was entered into the system on average when the front bumper was 1.2 m before the trigger pole with a scatter of ± 30 cm.

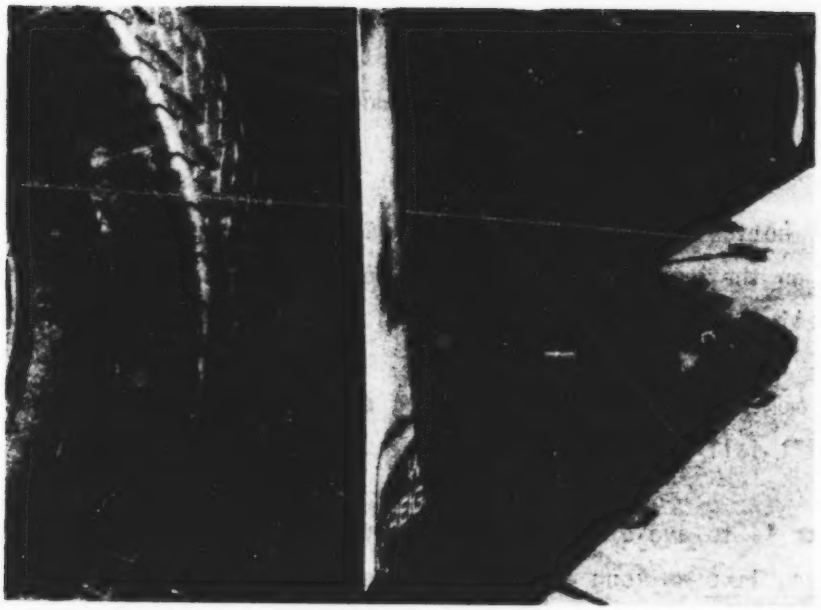

Figure B.1/ Pole Trigger Ultrasonic Sensor

APPENDIX C/ Instructions to Drivers

C.1/ Preliminary Barricade Trials

This experiment will examine your ability to avoid an obstacle that suddenly appears in the path of your truck.

The runway in front of you has been made into a two-lane roadway. The orange cones mark the left edge of the pavement and the white line marks the centreline. The right pavement edge is marked by the broken line.

On my signal, accelerate to about 50 km/h (.... rpm) and maintain a steady speed by driving in 5th gear (over range) on governor. Attempt to maintain your lane position as closely as possible. Also, be sure to maintain your normal viewing pattern down the roadway as much as possible.

You will notice the row of barricades located along the shoulder of the roadway on the passenger side. Each barricade has been set in the vertical position.

At some moment, while you are driving down the lane, one of the barricades will fall across your path.

Your task is to avoid hitting the barricade. You may do this <u>in any manner you like</u> as long as you don't leave the two-lane roadway that has been marked off.

Once you have avoided the barricade, drive down to the end of the solid white line, make a slow turn to the right, and drive back to this location. Once you arrive back here, stop facing south (experimenter to point out south) and wait for my signal to start.

On my signal, turn the truck around and accelerate for a second time to 50 km/h in this lane toward the barricades. Again, one of the barricades

will fall into your path and you will attempt to avoid it in any manner you wish as long as you remain in the two-lane roadway that we have laid out.

QUESTIONS ? ? ?

C.2/ Initial Barricade Training Trial

To recap the information we gave you earlier, this experiment will examine your ability to avoid an obstacle that suddenly appears in the path of your truck.

The runway in front of you has been laid out as a two-lane roadway. The orange cones mark the left edge of the pavement and the white line marks the centreline. The right edge of the pavement is marked by the broken line.

On my signal, accelerate in the right lane, the one closest to the barricades, to 50 km/h driving in 5th gear (over range) on the governor, with the accelerator depressed all the way. You may drive faster while distant from the barricades but you should be on the governor at a steady speed by the 1st pylon. You must maintain your normal lane position and also maintain your normal viewing pattern down the roadway.

Four events could take place as you drive down you lane. First, a barricade could fall in front of you as it did earlier. Sometimes the barricade will fall 30 or 40 m in front of you giving you plenty of time to react. Other times it will fall much closer to the truck giving you less time to react. In either event, your task is to avoid hitting the barricade by driving into the adjacent lane. Imagine, when you change lanes to avoid the barricade, that there is oncoming traffic in the adjacent lane, so you must get back into your own lane as soon as you can, once you've passed the downed barricade.

Once you've re-entered your lane, continue to the end of the solid white line marking the end of the course. At all times keep the accelerator fully depressed and do not use any brakes. At this point slow, turn to the right and return to the south end of the runway park facing south and await further instructions. Do not attempt to look back at the course.

The second event that could occur as you drive down your lane is that the barricade is already down across your path. Treat the downed barricade as you would any other obstacle blocking your lane and drive around it. Remember, there is oncoming traffic, so you want to spend as little time as possible in the adjacent lane. Once you are around the barricade, continue down the course on the governor to the end of the white line.

The third event that could occur is that you will be told exactly what barricade will fall in front of you and when it will fall. Treat this event in the same way you treated the first two.

The fourth event that could occur is that NO obstacle will fall in your path for the entire length of the course. This event has been included so you won't begin to anticipate a barricade falling near each end of the course. In this event, drive to the end of the line on the governor.

REMEMBER, IT IS IMPORTANT NOT TO USE THE BRAKES DURING THE TASK UNTIL YOU REACH THE END OF THE COURSE. KEEP THE ACCELERATOR DEPRESSED THROUGHOUT. HOWEVER, IF YOU BELIEVE THAT THE TRUCK IS OUT OF CONTROL, OR THAT YOU ARE ABOUT TO DRIVE OFF THE ROADWAY THAT WE'VE MARKED OFF, TAKE ANY ACTION NECESSARY TO REGAIN CONTROL AND COME TO A HALT.

QUESTIONS ? ? ?

C.3/ Subsequent Barricade Training Trials

Your task today is the same as it was the last time you participated.

Remember, on my signal accelerate to about 50 km/h and drive on the governor in 5th gear (over range) from the start to the end of the solid white line.

Recall as well, that one of the barricades might already be across your lane when you start the trial; or it may fall as you approach it, sometimes very near to the truck, other times further away; or perhaps none of the barricades will fall during a run; or you may be told which barricade will fall.

If you have to avoid a barricade, steer into the adjacent lane, but try to spend as little time as possible in that lane.

After you have passed the barricades, continue on the governor to the end of the white line before you slow for the turn.

FINALLY, IT IS IMPORTANT THAT YOU DON'T TOUCH THE BRAKE CONTROLS DURING THE TRIALS UNLESS IT IS NECESSARY.

QUESTIONS ? ? ?